SYSTEM ANALYSIS OF LOX/LNG EXPANDER BLEED ENGINE 'LUMEN'

Master's thesis

DLR German Aerospace Center
DLR German Aerospace Center
Institute of Space Propulsion
Stefan Schlechtriem
Langer Grund
74239 Hardthausen
Germany
Tel: +49 6298 28-203
Fax: +49 6298 28-190
Web: https://www.dlr.de/ra/en/

Malte Andreas Reitemeyer
Mail: malte.reitemeyer@stud-mail.uni-wuerzburg.de

Document Identification:

Title	System analysis of LOX/LNG Expander Bleed Engine 'LUMEN'
Subject	LUMEN
Author(s)	Malte Andreas Reitemeyer
With contributions by . .	
Last saved by	Malte Andreas Reitemeyer
Last saved on	2nd May 2023

Abstract

For the design, control and optimization of a chemical rocket engine, a thorough understanding of its behavior is needed. A complex interplay between combustion, fluid dynamics and mechanic components needs to be balanced. A system analysis is the basis for such an understanding, providing needed information for control strategies, and allowing predictions about the effects of changes to the system. For the technology demonstrator LUMEN such an analysis is used to evaluate its performance and identify areas for improvement. Within the scope of this thesis, existing models are compared to new engine test data to assess their validity. Due to deviations the existing models were improved and subsequently used to extrapolate the engine's behavior to other operating conditions. With these, additional points of interest for future tests can be identified, alongside with bottlenecks for improvement of the engine. Finally the controllability of different variables using various subsets of valves was explored.
It was found that in its current state, the maximum pump pressure of 150 bar limits LUMENs operational range most significantly. The operational flexibility for the nominal working point is in turn majorly constrained by the coolant mass flow requirement.

3. Improvements of the digital model **27**
3.1. Valve model 27
3.2. Heat flow 31

4. System Analysis **33**
4.1. Operational range 35
4.2. General 38
4.3. At nominal working points 41
4.4. Injection Temperature 45

5. Control Analysis **49**
5.1. Reduced valve sets 49
5.1.1. Turbine-controlled (TFV, TOV) 49
5.1.2. With mixer (FCV, TFV, TOV) 52
5.2. Control effects of valves 55
5.2.1. FCV 55
5.2.2. OCV 56
5.2.3. TFV 56
5.2.4. TOV 57
5.2.5. XCV 58
5.2.6. BPV 58

6. Conclusion and outlook **59**

Appendix **I**
I. Used symbols I
II. Abbreviations III
III. References IV
IV. Acknowledgements VI

1. Basics of chemical rocket engines

At the core of every rocket lies its engine. It produces the thrust needed to lift the rocket and accelerate it into orbit. In most orbital rockets this is a reaction engine based on chemical combustion, as these offer sufficient thrust to overcome earths gravity. Their design and optimization however is particularly complex, as they consist of various subassemblies and components who's interplay and dependency have to be considered.

1.1. Working principle

Reaction engines propel the vehicle through expulsion of reaction mass, following the principle of Newton's third law, "Every action has an equal and opposite reaction". The acceleration of mass backwards causes the vehicle to accelerate forwards. This acceleration is achieved by conversion of some kind of stored potential energy to kinetic energy. In case of chemical engines, this is the chemical energy contained within the propellants. Mono-propellant engines use a single propellant, releasing its energy through decomposition over a catalyst. In contrast bi-propellant engines use two propellants, a fuel and an oxidizer, which are combined in a thrust chamber and combusted [9][1]. These reactions release heat, increasing the pressure within the confined space. The resulting high-pressure gases are then released and accelerated through a nozzle, increasing their exit velocity.
This leads to two important values to consider for an engine, who's priority has to be weighed against one another: Thrust and specific impulse. The thrust force

$$F_t = \dot{m}_e v_e^* \tag{1.1}$$

dictates the force and thus acceleration applied to the rocket and depends on the exhaust mass flow $\dot{m}_e$ and the effective exhaust velocity v_e^*. It is especially critical for the first stage,

[1] p.154

which needs to overcome earth's gravity. The specific impulse

$$I_{sp} = \frac{F_t}{\dot{m}_t * g_0} \tag{1.2}$$

depends upon the thrust force and total mass flow $\dot{m}_t$, with g_0 as standard gravity. It is a measure of efficiency, how much velocity change is achieved by a given mass of fuel [9][2]. This is most important for upper stages, to reduce the fuel, and thus total mass, needed to transport a certain payload into its desired orbit [9][3].
Thrust and specific impulse stand in competition, as any given engine has a finite amount of available power. For ease of explanation assume an engine with $\dot{m}_t = \dot{m}_e$ and $v_e^* = v_e$. The kinetic energy of the exhaust is given as

$$P_{kin,e} = \frac{1}{2}\dot{m}_e v_e^2 \tag{1.3}$$

with $\dot{m}_e$ the exhaust mass flow and v_e the exhaust velocity. Given a constant energy per second, a doubling in the exhaust velocity would allow only for a quarter of the mass flow, which in turn would result in half the thrust.

$$P = const. \Rightarrow F \propto \frac{1}{I_{sp}}$$

As such, to achieve both sufficient thrust and efficiency to reach orbit, megawatts to gigawatts are needed, necessitating the high energy density of chemical propellants. High flow rates, temperatures, and pressures are still needed even with chemical propellants. [9][4]

1.2. Components

To enable and endure these demanding conditions, various components are needed. These are commonly grouped into assemblies. While the basic design and layouts are similar for many engines, the specifics can vary and are optimized to each engine design individually. In following, the most commonly seen components and those relevant to the further work are explained in further detail.

[2] p.155
[3] p.156
[4] p.155

1.2.1. Thrust Chamber Assembly (TCA)

The central component of a rocket engine is the thrust chamber assembly, in which the propellants are injected, mixed, combusted and subsequently expelled. It is comprised of multiple parts: the injection head, the igniter, the combustion chamber, its associated cooling channels, and the nozzle [9][5].

Injector

The injector is responsible for injecting the propellants into the combustion chamber. The objective here however is not limited to simple injection, but also includes rapid and even mixing through atomization to achieve an even and complete reaction within the three-dimensional combustion zone. This is crucial to maximize the chemical energy released, as well as preventing damage to the combustion chamber and the injector itself. Regions of elevated temperature, caused by a higher combustion rate and density, or an excess of oxidizer, can cause excessive wear if in contact with the chamber walls or the injector face. In contrast, in the case of using carbon-rich fuels, an excess of fuel might cause coking, altering the geometry or even clogging parts of the injector [12].
To accomplish a homogeneous mixture, various injector types exist [4] [9][6]. Simple parallel injector nozzles rely upon convection and turbulence for mixing, and are rather inefficient. An impinging injector uses angled injector nozzles to cause a collision of the resulting streams. These injectors produce a fan or cone of atomized propellants, depending on the geometry. In the simpler form the propellants from all involved nozzles are identical, named a "like impinging injector". A more complicated design is the "unlike impinging injector" where both fuel and oxidizer are injected together in intersecting streams. This design improves initial mixing, though sufficient mixing is still possible with the simpler like impinging injectors.
The swirl injector supplies the propellants tangentially into the channel, creating a rotating flow inside. The resulting cone of propellant is spread apart by centrifugal force as it exits the injector. Improving upon this design, the coaxial swirl injector adds a second cylindrical cavity around the first, into which propellant is also injected tangentially, resulting in a second cone coaxial with the first. Most commonly, the two cones are unlike, consisting of oxidizer and fuel. By tuning the expansion angles of the resulting cones, they can be made to intersect, causing mixing and further atomization of the propellants.
The coaxial sheer injector does not utilizing a swirl, instead relying upon the differing exit velocities and densities of the two propellants to ensure sufficient mixing. As it does not

[5] p.167
[6] p.163-166

require tangential supply, it is easier to machine and produce.
Porous injection offers a different approach entirely, as it does not have distinct injectors, but instead evenly injects one or both propellants across a large area. This is accomplished by using a porous material through which one of the propellants can seep, allowing for this diffuse injection. To avoid mixing of the two propellants prior to injection the other propellant is commonly transported through more conventional, distinct, injectors within the porous material, being released at the face of the injection area.

Igniter

Hypergolic propellants do not require an additional igniter, but suffer from other downsides covered in section 1.4.1. Unlike hypergolics most propellant combinations do not combust when simply mixed, but need an ignition source. This ignition source can be either single- or multi-use and can be internal or external to the engine [13][7].
The simplest form of ignition when using non-hypergolic propellants is a pyrotechnic igniter. This, for example, can be a flare placed inside the combustion chamber and remotely activated at startup, igniting the propellant mixture as it comes into contact. Inherently this is only usable for a single ignition, and is mainly viable for engines that are ignited on the ground, not during flight.
Another relatively simple way is to utilize the ease of hypergolic ignition, but only on a small scale. To trigger ignition, a small amount of a third substance is injected into the combustion chamber, which is hypergolic with one of the main propellants, igniting itself, and subsequently the main propellants as they mix. Common substances used for this are triethylaluminium (TEA) and triethylborane (TEB) [15], jointly referred to as TEA-TEB. While multiple ignitions are possible with this by injecting only controlled portions of it for each ignition, the number of available ignitions is still finite, and the risk of handling is still present, though significantly reduced.
While spark plugs might seem attractive since they are found in cars for the same purpose, the turbulence and harsh conditions within the combustion chamber make direct ignition by a spark plug unreliable and destroy it quickly during operation of the engine. Instead the spark plug can be used in a more controlled environment slightly outside the combustion chamber to ignite a pilot flame. This torch flame then fires into the chamber, leading to ignition while keeping the spark plug in a safer position. This allows for a theoretically arbitrary number of relights of the engine.
More recently a new igniter type based on lasers has been developed and tested. A high power pulsed laser is discharged into the combustion chamber for ignition. The high energy density heats a small volume of propellant to very high temperatures, igniting it in the

[7] p. 234

process. Due to the small focusing area and short pulse time, only a small amount of energy is needed to achieve a sufficient temperature for ignition. In combination with advances in laser and battery technology, this kind of ignition system can easily be integrated into a rocket engine.

Combustion chamber

The geometry, especially diameter, length and throat area of the combustion chamber, has a major impact on the combustion dynamics within it. As its mass is a large portion of the total mass of most engines, reducing the chamber size and thus mass is imperative. The length of the combustion chamber determines the time frame in which the chemical reaction has to occur. Insufficient chamber length thus may inhibit complete combustion. Meanwhile the diameter of the chamber correlates to the heat flux to the walls. Additionally, as it contains a continuous combustion at high pressures and temperatures, the combustion chamber needs to be highly resilient. On the one side, it must be structurally sound to withstand potentially hundreds of bar of pressure [13][8], depending on the design. On the other, heat fluxes in the range of megawatts [9][9] get emitted by the combustion gases before they can be ejected. This poses a challenge for cooling while keeping mass low, especially because most materials weaken with heat.
The heat load itself can be reduced through insulating and ablative coatings. Ablative coatings slowly burn away during operation, forming a protective sacrificial layer. This inherently limits the engines service life and in addition alters the geometry of the chamber gradually as it gets consumed, changing the combustion dynamics. Furthermore, uneven heat distribution, like hot spots, can lead to a faster burn rate in some places, ultimately risking a burn through and failure of the chamber.
The simplest cooling method is the radiatively cooled chamber. To achieve this the chamber is allowed to reach its equilibrium temperature at which the heat influx is being matched by the thermal radiation emitted by the hot chamber. This requires high wall temperatures, which requires specialized metal alloys for the chamber, alongside lower chamber pressures to account for the heat-related lower structural strength.
An alternative option to this is regenerative cooling, which utilizes the propellant as a coolant prior to combustion. To accomplish this, it is routed through cooling channels within the chamber walls, where it absorbs heat from the surrounding material. Cryogenic propellants are favorable for this type of cooling, due to their low temperature, but not required. While this extends lifetime significantly, it requires a more complicated manufacturing process to include the channels in the solid chamber structure. This also introduces a further

[8] p.226
[9] p.169

pressure loss prior to the injector, requiring higher pump pressures, as well as creating interdependency between cooling and propellant feeding, complicating control.

Cooling channels

Cooling channels run inside the combustion chamber walls, allowing coolant to absorb the heat deposited by the combustion. The manufacturing and layout has a wide range of possibilities. The materials used in both the chamber and channels must maintain structural strength at high temperatures, while also being highly thermally conductive. Commonly copper or a nickel alloy are used for this purpose. Secondly the coolant can either flow in the same direction as the gases inside the combustion chamber, named co-flow, or against, named counter-flow. The cooling channels inside may be purely longitudinal, be arranged in a spiral, or may not be distinct channels at all. The simplest arrangement is a secondary hull around the combustion chamber to fully surround it with coolant. Heat transfer and structural strength of the chamber are comparatively low, and insufficient for higher power engines. Instead, to increase the effective surface area and provide structural support, the cavity is segmented by walls into separate channels. This can be accomplished in four main ways. [7]
A corrugated metal sheet can be sandwiched between and fused to the outer and inner wall, creating semi-circular channels in between, and providing high structural strength.
As another option, the chamber is directly constructed from tubes, later serving as coolant channels. Fusing a large number of these tubes together forms a continuous chamber wall. This results in a slightly uneven inner wall.
Alternatively the chamber can be machined from a solid metal piece, usually copper, and channels machined into the side (Figure 1.1a). This allows for more complex channel geometries that vary along the length of the chamber, but is more labor-intensive and thus costly. Afterward machining the channels are closed through electro-deposition (Figure 1.1b), and then coated with a structurally reinforcing layer.
By additive manufacturing conventional cooling channel designs can be built as a solid piece in one print. But also even more complex cooling structures, such as a continuous outer chamber filled and reinforced with a lattice between the outer and inner wall can be used.

1.2.2. Nozzle

Downstream of the combustion chamber, a nozzle is utilized to efficiently convert the high temperature and high pressure gases produced within the combustion chamber to

(a) **After machining of the channels**

(b) **After closing of the channels**

Figure 1.1.: **Combustion chamber of LUMEN during manufacturing [6]**

a directed high speed gas flow. To convert the thermal energy and pressure into kinetic energy, a converging-diverging de Laval nozzle (see Figure 1.2) is used.
Starting from the cylindrical combustion chamber, the cross-sectional area is gradually decreased, increasing the flow speed of the escaping gases. Eventually, the flow speed reaches the speed of sound of the gases, leading to a choked flow condition. Further narrowing the diameter would only increase the pressure upstream, but not push beyond the speed of sound. However, expanding the cross-sectional area lets the pressure decrease further, as the gases get accelerated beyond the speed of sound, increasing the impulse imparted upon the engine. The final exit velocity

$$v_e = \sqrt{\frac{TR}{M}\frac{2\gamma}{\gamma-1}\cdot\left(1-\left(\frac{p_e}{p_i}\right)^{\frac{\gamma-1}{\gamma}}\right)} \tag{1.4}$$

is calculated based upon the gas temperature T, molecular mass of the gas M, universal gas law constant R and isentropic expansion factor $\gamma = C_p/C_v$, alongside the pressure at the nozzle inlet p_i and nozzle outlet p_e. The temperature, molecular mass and inlet pressure can vary depending on the chamber conditions, while the pressure ratio from inlet to outlet depends on the ratio between throat area and nozzle area.
There are multiple trade-offs to be made here. The first one also relates to the combustion

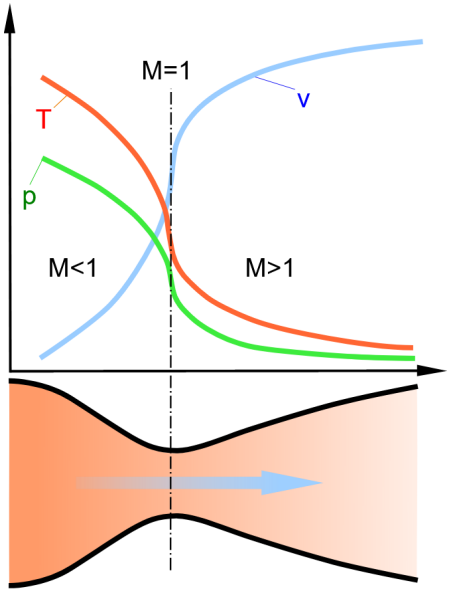

Figure 1.2.: **Diagram of a de Laval nozzle [21]**

chamber, as a higher pressure at the throat with constant mass flow increases the efficiency, but also the chamber pressure, and subsequently overall system pressure. This complicates the design and results in a heavier engine. The pressure at the throat depends on the throats cross section relative to the mass flow.
Secondly, the wider the final area of the diverging part, the lower the final exit pressure, and consequently the higher the exit velocity. This however requires an ever larger nozzle, making for a heavier and larger engine, with ever more diminishing returns. While a lower exit pressure isn't an issue in the vacuum of space, for engines used at sea level, exit pressures below one bar can allow the surrounding atmosphere to push into the nozzle. This causes the separation of the gas flow from the nozzle walls, which in turn leads to instabilities, oscillations and transient forces large enough to damage the engine.
First stage engines therefore use a comparatively smaller nozzle, avoiding flow separation and giving space for multiple engines to be mounted, increasing total thrust. Engines used on upper stages commonly have a nozzle as large as feasible, making full use of all available space for maximum efficiency.

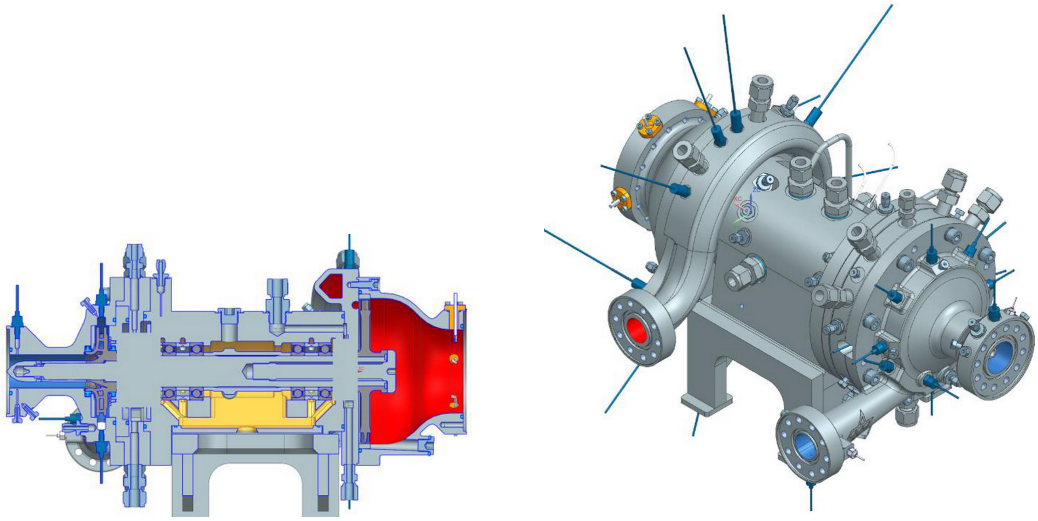

(a) **Cross section with pump in blue, shaft unit in yellow, turbine in red**

(b) **3D render with pump on the right, turbine on the left**

Figure 1.3.: **LUMEN's fuel turbopump [19]**

1.2.3. Turbopump Assembly (TP)

To inject the propellants into the high pressure environment of the combustion chamber, they must be at a higher pressure themselves. While this could be achieved by storing the propellants at high pressures, this is not practical beyond a certain point, since this would require increasingly heavier tanks to contain ever higher pressures, increasing the structural mass of the rocket. Instead pumps are used to raise the pressure of the propellants prior to their injection into the engine. As a power source most pumps use a turbine, leading to the combined term of a "turbopump".

Turbine

The demands on the turbine vary strongly depending on what is used as a medium. This mainly depends on the cycle (see 1.3). In designs where combustion gases are used, they could either be fuel-rich, or oxidizer-rich. The later sets higher demands on the material used, as heated excess oxidizers react with most metals and alloys. On the other side, if carbon-containing fuels are used, a fuel-rich mixture may cause coking, clogging downstream components with carbon deposits.

In either case, a compact and lightweight design is desired to minimize the mass of the engine, while also maintaining a high efficiency. This favors small, high speed turbines, with minimal tolerances, as even small deviations may lead to significant drops in efficiency in one direction, and destruction of the turbine in the other. This sets high demands on the manufacturing precision and material choices.

Sealing

The mechanical connection between the turbine and pump must still withstand high angular speed and torque. Additionally, depending on the propellant and cycle, there may be a temperature gradient of many hundreds of Kelvin between the pump and turbine. Still more importantly though, the turbine may contain fuel and the pump oxidizer, or vice versa [2] [5]. Leaking along the shaft has to be prevented. The cryogenic environment along with the exposure to oxidizers on one side makes the use of grease- or rubber-based seals challenging. Tight-tolerance interlocks made of metal and carbon are therefore preferred. Additionally, the cavity may be pressurized with an inert gas, to block the path of leakage with higher pressure.

Gearing

As the operation regime of the turbine might be mismatched with the operation regime of the pump, gearing may be needed to adjust the rotational speed. This is especially needed in a combined turbopump, where one turbine drives both the fuel and oxidizer pump. These usually have far different requirements, as they pump different media at different pressures and mass flow rates. Avoiding gearing to save mass can be done through joint design of the pump and turbine, matching their operational and optimal regimes. However, this can impact efficiency and makes the development process more complicated.

Pump

To facilitate a high mass throughput and pressure rise in a small form factor, a high-speed centrifugal pump is commonly chosen. From a comparatively low pressure in the tank, the medium enters the pump in the center of the impeller, from where it gets accelerated radially outwards. A static diffuser, comparable to a ring of nozzles, is often used in converting this velocity into increased pressure, before the propellant is discharged from

the pump into the remaining engine plumbing [7].
Similar to the turbine, tight tolerances are needed to keep the efficiency high, as the large pressure rise across the oftentimes single pump stage quickly causes backwards leakage and turbulences. Furthermore, the sharp pressure rise can lead to cavitation along the edges of the impeller, reducing lifespan and efficiency. To mitigate these issues, the pressure rise can be split across multiple pump stages. That way the individual stages can also be optimized for the respective pressure regimes. The increased efficiency oftentimes does not account for the increased development time and mass required. One of the exceptions is an axial inducer upstream of the main stage, serving to raise the inlet pressure, reducing the pressure differential. A second exception is in the case of liquid hydrogen, the low density of which makes multiple stages necessary.

1.2.4. Gas generator / Preburner

Describing a secondary combustion chamber for the production of heated combustion gases, gas generators and preburners are quite similar. If the resultant gases are injected into the main combustion chamber afterwards, it is called a preburner, while if they are eventually expelled in a different manner, it is called a gas generator. For simplicity 'gas generator' is used in this section to refer to both.
As mentioned before, the propellant pumps have a high power demand [7]. While in some modern engine designs this is provided by batteries, most utilize a turbine to source it from heated propellant or combustion gases. Those combustion gasses are often produced within a dedicated gas generator. As the resulting gases will get in contact with further components afterwards, and to avoid the need for active cooling, temperatures as high as in the main combustion chamber are undesired. To achieve a balance between efficiency and a low combustion temperature, the ratio of fuel and oxidizer is non-stoichiometric, leading to either a fuel-rich or oxidizer-rich exhaust. This further categorizes the type of gas generator utilized in an engine.
Similar to a main combustion chamber, a gas generator includes injectors, though typically no nozzle or cooling is present, as the gases are routed through pipes to the turbines.

1.3. Cycles

The method by which propellants are delivered into the combustion chamber is crucial for the design of an engine. These different concepts are called 'cycles', and the most common cycles are described in the following:

1.3.1. Pressure-fed

In the simplest cycle, non of the engine components raise the pressure of the propellants or actively feed them into the combustion chamber. Instead, the propellant is already stored at elevated pressures in the main tanks, from which it is released into the engine. Typically, an inert gas like nitrogen or helium is injected into the tanks as propellant is drained to maintain pressure. This type of feed system dramatically simplifies the engine, as no pump is needed. The overall reliability of the engine is also increased, as it reduces the points of failure drastically. A faster on-off cycling is enabled as there is no moment of inertia from a pump assembly. However, it increases the structural mass of the rocket, as the tanks need to be heavier to withstand the higher pressures inside. Furthermore, efficiency increase is limited, as at some point any increase by higher tank and chamber pressure is lost to the increased structural mass required. The Aestus and Draco engines are examples of this cycle, as is the AJ-10 [20][17][3].

1.3.2. Electric pump

A recent development is the option of an electric motor powered by batteries. This is enabled by advances in battery technology, enabling sufficiently high power and energy densities. Utilizing this avoids the development of a turbine and its associated components while still taking advantage of an increased pressure level inside the engine. A certain amount of mass is still used just to power the pumps, though in the form of batteries rather than propellant. While it may be advantageous in small engines, as efficiency in turbopumps is ever harder to maintain at smaller sizes, the amount of batteries becomes detrimental with larger engines and rockets. The Rutherford engine is one of the most prominent examples of this cycle [1].

1.3.3. Combustion tap-off

The combustion tap-off cycle diverts a fraction of the exhaust gases from the combustion chamber to power the turbines. This however has some drawbacks and difficulties. An additional exit from the combustion chamber significantly complicates design and manufacturing process of the chamber and its cooling channels. It also can negatively impact the flow pattern within, leading to an unstable and asymmetric combustion. Additionally, the gases from the combustion chamber typically have significantly higher temperatures and pressures than those of a gas generator. This increases the strain on both the piping and

the eventual turbine. Directly coupling the turbine power to the combustion chamber can also cause unwanted interactions. By the very nature of this cycle, the turbine gases also can not be reinjected into the combustion chamber, as they have a lower pressure.
This cycle does however save the mass and development effort of a gas generator, while still exploiting the efficiency of a turbopump. One of the most prominent examples of this cycle is the BE-3 engine [18].

1.3.4. Gas generator

As explained in section 1.2.4, most commonly the turbine gases are produced within a separate combustion chamber. If these are then subsequently not injected into the main combustion chamber, it is a gas generator cycle. The portion of propellant not used in the main combustion chamber leads to a reduction in efficiency. Despite this there are a number of advantages to this compared to a preburner (see Section 1.3.5).
Most importantly, the exit pressure from the turbine can be as low as ambient pressure, instead of being higher than chamber pressure. This enables a lower pressure level and consequently milder conditions within the turbine and the gas generator. Additionally, the propellant system upstream of the gas generator does not need to be at an elevated pressure as well, as the injection pressure to the secondary combustion chamber is usually lower than that of the main chamber. This lowers the requirements for the pumps and pipes, reducing the mass of the entire engine. The loss of efficiency can also be slightly reduces by expelling the turbine exhaust through a separate nozzle, producing additional thrust.
Since the turbine exhaust does not get injected into the combustion chamber, it does not need to match the main propellants. As such the gas generator may use a different propellant mix that is more advantageous in the gas generator, but not in the main combustion. Either due to a low performance, or issues of price or hazardousness. Alternatively, the gas may be generated by catalytic decomposition, similar to a mono-propellant engine.
If the gas generator propellant is different from the main propellant it is almost always stored at high enough pressure for injection. An additional pump for the small volume of gas generator propellant would not be worthwhile. Examples for this variation are the A7 engine and RD-107, using hydrogen peroxide decomposition to generate steam [8][10]. Engines like the Merlin and the F1 are cases of utilizing the same propellant as the main chamber in a gas generator, both running fuel-rich [17] [8][11].

[10] p.39
[11] p.7

1.3.5. Staged combustion

This name refers to the multiple stages of combustion where a preburner is used with subsequent injection of the turbine exhaust into the main combustion chamber. While it is more complex and increases the demands on the propellant system, the higher efficiency of routing the turbine exhaust back into the combustion chamber may justify this design decision, especially in high efficiency engines. The re-injection harnesses the remaining available energy after the turbine, reducing energy losses. Examples of a simple staged combustion cycle are the RS-25, running fuel-rich, and the BE-4, running oxidizer-rich [8][12] [14].
A specific variant of the staged combustion cycle is the full-flow staged combustion cycle. In this, all of the propellant runs through preburners, one oxidizer-rich, the other fuel-rich, and subsequently through their respective turbopumps, before being injected into the main combustion chamber. This avoids the issues of unintended mixing by leakage between turbine and pump, while also decreasing the temperatures in the preburners and turbines. In turn, these need to handle a higher mass flow rate. Most importantly, the challenges of both a fuel-rich and an oxidizer-rich preburner and turbine need to be handled, essentially forming two staged combustion cycles within one engine. Along with this comes a mass increase from the two turbines and preburners. Nonetheless, this can increase the lifetime and durability of the engine. The pre-heating and pre-mixing prior to injection into the main combustion chamber also improves both injection itself and the subsequent combustion. An example of this cycle is the Raptor engine [16].

1.3.6. Expander

Instead of using both propellants to produce hot combustion gases, the heat produced by the combustion chamber can be utilized. With this, one or both propellants are heated and "expanded" before being directed towards the turbines. This can be realized in various forms.
What all of these variants have in common though is that the pumps are powered by the heat absorbed by the combustion chamber walls. This harnesses the "lost" energy while also avoiding the need for a second combustion chamber. However, this inherently limits the size and power of any closed expander engine. As the size of the main combustion chamber and subsequently propellant injection mass increases, the combustion volume, and thus injection volume, increases by the cube of the radius of the combustion chamber. Meanwhile the heat absorbed on the surface increases with the square of the radius, eventually leading to insufficient heat to feed enough propellant. This boundary is estimated within the realm of

[12] p.11

hundreds of kilonewtons [11].
Both the combustion chamber and the nozzle extension can be used as heat sources, and the fuel, the oxidizer, or both can be used as the medium. Furthermore either all the propellant can be routed to be heated, or only a portion of it. The "classical" closed expander bleed cycle first heats the fuel around the combustion chamber, then heats it further in the nozzle extension, before utilizing it in the fuel turbine and afterwards in the oxidizer turbine. Further variations of this cycle employ using the oxidizer instead of fuel, having a joint turbine for both propellant pumps, or changing the flow order between chamber and nozzle. The RL-10 for example uses this type of cycle, with a joint turbine [8][13].
As forcing all the fuel through the cooling channels requires a high head pressure, and not all of it is needed to run the turbines, the split expander cycle only uses a portion of the entire fuel to heat and power the turbines. A large portion gets directly pumped into the main combustion chamber, reducing the pump power required. This does however raise the operating temperature of both the cooling channels and the turbines, setting a minimum to the mass flow to avoid damage.
To avoid the leakage risks mentioned before, two separate turbines could be powered by their respective propellants. One is typically heated with the combustion chamber, the other in the nozzle extension, though it is also possible to heat both propellants equally around the chamber as well as the nozzle extension. This is the dual expander cycle. It slightly increases complexity in the cooling piping while avoiding complexity in the turbopump seals. The propellant sides can also be split, either just one or both, leading to the dual split expander cycle.

1.3.7. Expander-Bleed

A way to circumvent the thrust limitations of a closed expander cycle is to vent the turbine exhaust instead of injecting it into the combustion chamber. Similar to an open gas generator, this allows for a lower exit pressure of the turbines, and subsequently lower pressure throughout the propellant system. This also decouples the fuel injection from the turbine, enabling higher thrust at the cost of lower efficiency through propellant bypassing the combustion chamber. As this decoupling allows for significantly higher chamber pressures, the resulting increase in efficiency makes this cycle comparable to closed expander cycles. Examples of this engine are the LE-9 [10] and LUMEN.

[13] p.42

1.4. Propellant combinations

Alongside the chosen cycle, the choice of propellant is crucial to the design and core parameters of an engine. Different propellant combination have certain maximum possible specific impulses, as well as their own challenges.

1.4.1. Hypergolics

A major upside of hypergolics is their ease of ignition, not requiring a separate igniter. This also enables high cycle frequency, ideal for attitude control. Additionally they are storable for long durations, making them useful for orbital maneuvering thrusters on satellites. However hypergols also have a lower efficiency, as the molecular mass of the exhaust is higher, and temperature usually lower. The storage density is relatively high, allowing for small tanks and low structural mass. Hypergolics are also highly toxic, making them dangerous and difficult to handle.

1.4.2. Kerolox (RP-1/LOX)

RP-1 is a further refined variant of kerosine, a mixture of medium length hydrocarbons. It has a high density and is liquid at room temperature, making storage and handling comparatively easy. The efficiency is better than for hypergolics, but not the best, due to the high percentage of carbon dioxide to water in the exhaust increasing its average molecular weight. Due to this high carbon content, fuel-rich mixtures can cause a carbon build-up from incomplete combustion called coking, clogging piping and components.

1.4.3. Hydrolox (LH2/LOX)

Hydrogen is a carbon-free fuel, preventing coking and decreasing the molecular weight of the exhaust, increasing efficiency. For chemical bipropellant rockets, this combination achieves the highest specific impulse. Its combustion products, water and excess hydrogen, are very light molecules and the reaction releases a large amount of energy per molecule. Due to its very low density and boiling point, storage of hydrogen is demanding, requiring large tanks with thick insulation. Similarly, the low density requires complex multistage pumps and high performance seals.

1.4.4. Methane/LNG (CH4/LOX)

Methane is the lightest hydrocarbon, taking advantage of a higher storage density compared to hydrogen while keeping a higher efficiency than kerosine. While coking is still possible, it is less common. Methane needs to be stored cryogenically, but is similar in boiling point to liquid oxygen.

2. LUMEN

LUMEN (Liquid Upper Stage Demonstrator Engine), is an expander-bleed cycle engine, powered by liquefied natural gas (LNG) and liquid oxygen (LOX). This propellant combination is relatively new for rocket engines, but promises a "best of both worlds" compromise between kerosene and liquid hydrogen.
The LUMEN engine uses the modular approach of a breadboard engine, where individual components can easily be altered and exchanged for others, allowing for faster and more segmented development of components. In a normal engine, all parts are optimized and tuned for one another, usually necessitating adjustments to all other components when one is changed. As such, to conduct tests on a new design for a sub-component all other components have to be adapted or newly developed. Instead of this, LUMEN aims to keep each part design as independent as possible, with broader operation margins, favoring modularity over efficiency and optimization.
For this engine mass and volume optimization are not a priority since it is a technology demonstrator. This results in a number of advantages like faster and cheaper development, testing new concepts and designs before mass-optimizing them. Swapping only a single component also allows for a more direct comparison than comparing two separate engines, resulting in more meaningful evaluations.
To allow for these wider performance margins and reduce the inter-dependencies of the components, the choice of the expander-bleed cycle is advantageous, and also fits the concept of an upper stage engine.

2.1. Architecture and components

The overview seen in 2.1 shows the layout of all the major components of the LUMEN engine. A two turbine arrangement with a separate fuel turbopump (FTP), comprised of LNG turbine and pump, and oxidizer turbopump (OTP), comprised of LOX turbine and pump, is used.

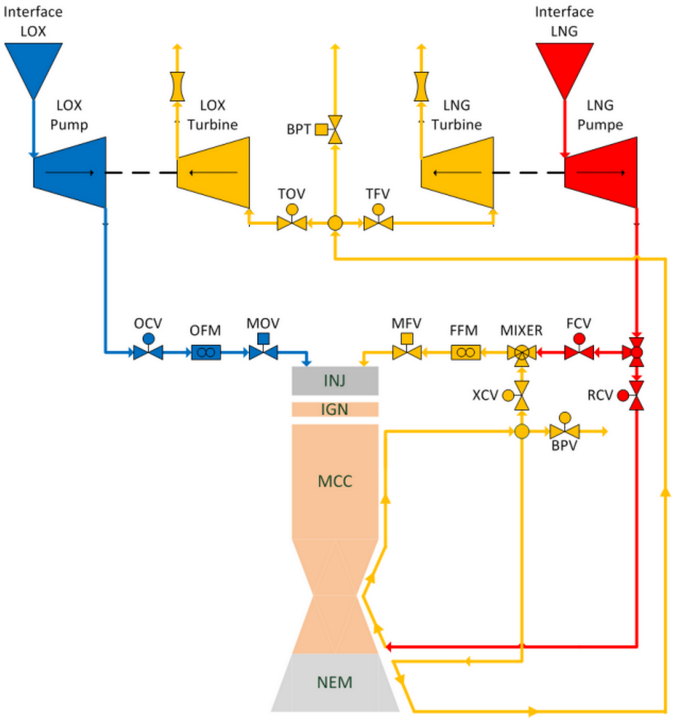

Figure 2.1.: **Flow schematic of LUMEN, oxidizer flow in blue, cold LNG in red, heated LNG in yellow, abbreviations explained in appendix I [19]**

2.1.1. Valves

The valves in the engine allow alterations of the flow paths and adjustment of the balance between coolant and injection, providing a greater variety of operating modes. The majority of valves are two positions open/closed valves such as the Main Fuel Valve (MFV) and Main Oxidizer Valve (MOV). The six valves explained in following (FCV, OCV, TFV, TOV, XCV, BPV) are able to be partially closed, allowing for fine control of the engine.
These control valves have two kinds of characteristics, describing how the cross sectional

area is related to the position. This also impacts the relation between the position and pressure drop across the valve.
Linear valves open linearly, meaning that every change in position changes the cross sectional area by an equal amount. Equal percentage valves open in an exponential shape, with larger increases the further open the valve already is. This results in every change in position having a proportionally equal change in cross sectional area.

FCV

The Fuel Control Valve has an equal percentage characteristic and is located between the fuel pump and the mixer. With it, the direct fuel flow bypassing the cooling channels can be controlled. Routing fuel this way avoids the additional pressure drop through the cooling channels, reducing the overall fuel pressure level required for operation.

OCV

The Oxidizer Control Valve has an equal percentage characteristic and is located between the oxidizer pump and the injector head. Closing it increases the pressure drop and subsequently requires a higher pressure level to maintain the same injection pressure. This allows throttling the oxidizer flow while keeping the turbopump speed constant.

TFV

The Turbine Fuel Valve has a linear characteristic and is located upstream of the fuel turbine, throttling the mass flow through it. Through this the power available to the FTP can be controlled, reducing or increasing the pump power. This in turn raises or lowers the mass flow and pressure rise across the fuel pump.

TOV

Similar to the TFV, the Turbine Oxidizer Valve has a linear characteristic and is located upstream of the oxidizer turbine, serving to control the power of the OTP, regulating the mass flow and pressure level of the oxidizer system together with the OCV.

XCV

The Crossfeed Control Valve has an equal percentage characteristic and is located between the outlet of the combustion chamber cooling channels and the mixer. This allows heated fuel to be passed over to the fuel injection, raising the temperature of the fuel. Additionally this allows for "recovery" of fuel after it has been used for cooling. This can be advantageous if more fuel is needed for cooling than for running the turbines.

BPV

The Bypass Valve is located behind the outlet of the combustion chamber's cooling channels, similar to XCV. Instead of mixing the fuel for injection, it is instead vented and discarded. While this expels fuel without it being used for thrust or turbine power, it allows for venting of excess cooling mass while avoiding raising the injection temperature, and keeping the turbine power stable to maintain the working point. As the highest efficiency likely necessitates keeping this valve closed, it was not included in the initial analyses.

2.1.2. Interfaces

Supply of propellants is enabled through the test stand interfaces. These can supply LOX and LNG at a range of temperatures and pressures, also allowing for tests without turbopumps or at lower power. They can also supply LN2 and GH2 for component tests, conditioning and purging. The values later used for the digital model interface are listed in Table 2.1

Table 2.1.: **Model interface parameters**

	Pressure (bar)	Temperature (K)
LNG	5	120
LOX	5	90

2.1.3. Turbopumps

To reduce interdependence, LUMEN utilizes separated turbopumps for fuel and oxidizer. Both the fuel turbopump (FTP) and oxidizer turbopump (OTP) are optimized for their

respective conditions. Nonetheless, both turbopumps use identical bearing assemblies to simplify development and maintenance as well as reduce cost.Both pumps are inducer-less centrifugal impeller pumps. Particularly notable is the "battleship" casing, designed to withstand damage and failures of the contained turbine and impeller safely, reducing risk during development and operation. The operational limits of the turbopumps will be elaborated in section 2.2.

2.1.4. Igniter

While initially a laser-based igniter had been planned, in its current configuration a state of the art torch igniter is used. This is a temporary change for improved reliability during development of other components of the engine, and may be reverted at a later point.
The igniter is mounted within a separate igniter ring at the upper end of the combustion chamber.

2.1.5. Injector

The injector used for the LUMEN engine is a set of coaxial shear injectors at the top of the combustion chamber. Also in consideration is a porous LNG injection, though this is not used in the current configuration. Motivation for this possible change is inconsistent flame anchoring, as in some operational regimes the main flame front shifts away from the injector face and further downstream inside the combustion chamber under some conditions. Resulting from this are incomplete combustion, unused combustion chamber space and reduced heat flux to the cooling fluid. A porous injector would likely anchor the flame reliably to the injector, preventing these issues.

2.1.6. Combustion chamber

For the combustion chamber an elongated copper chamber with counter-flowing cooling channels is used. The elongated shape is chosen to increase heat flow into the coolant and thus increasing power available to the turbines, which is a common feature in expander engines. High-aspect ratio cooling channels, meaning low width compared to height, are utilized. These increase heat transfer and efficiency, aiding to increase the heat flow to the coolant and limiting the wall temperature. The fuel used as coolant is kept in a super-critical state, which is favorable for stable heat transfer.

2.1.7. Nozzle extension

Currently, the nozzle extension of the LUMEN engine is comparatively small. The main utility of a nozzle extension is increasing efficiency, which is not the main priority at this time. However, the heat absorbed by the nozzle is used to further heat the coolant after it has passed through the combustion chamber cooling channels. This raises the temperature of the coolant later used in the turbines, increasing their efficiency.

2.2. Constraints

Analyzing the operational limits of the engine is of major importance. These red lines must not be crossed during normal operation. While some of these are hard set, most are cautionary estimates to avoid damage to any components, and may be extended once further testing confirms the viability.
The pumps and all the connected piping is rated up to 150 bar. This limitation could be expanded through the installation of components with a higher rating. However this is also a safety measure, and can not be altered at the current time.
As the turbines can only withstand a certain temperature, the gases driving the turbine should not exceed 700 K. While this number is not the precise limit resulting from the material properties, it is the current estimate with safety margin.
On the other side the entering gases need a certain minimum temperature dependent on the pressure to not liquefy inside the turbine. In practice, there is also a minimum temperature and pressure to enable stable flow within the turbine, though this is not explicitly modeled as a constraint. Instead, the computational model is unable converge for these conditions.
The rotational speed of the turbopumps must also be kept below 30000 rpm for the OTP and 57000 rpm for the FTP due to component rating and for safety reasons.
Furthermore both turbopumps have speed regimes which should be avoided during continuous operation, as unstable resonances at these points may be detrimental. This critical speed is around 18000 rpm, with a buffer of 500 rpm either side.
Concerning the the combustion chamber: To maintain critical conditions within the cooling channels, sufficient pressure must be maintained at all times. As the lowest pressure for the cooling channels is at the outlet of the nozzle extension, this is the important measuring point. The minimum pressure is at around 46 bar. To also maintain adequate cooling, there is a minimum coolant mass flow needed. This is dependent upon the heat influx, which is estimated through the chamber pressure, and the coolant pressure.
As was mentioned in section 2.1.5, flame anchoring has been identified as an issue with

the current injector configuration. The mode and effectiveness of the shear mixing at the injectors can be characterized with the momentum flux ratio J

$$J = \frac{\rho_{CH4} * v_{CH4}^2}{\rho_{LOX} * v_{LOX}^2} \tag{2.1}$$

with ρ_{CH4} and ρ_{LOX} the respective densities of methane and oxygen at the injector, and v_{CH4} and v_{LOX} the respective injection velocities. While the minimum value for stable flame anchoring is not clearly established, J should exceed 10 to ensure flame anchoring.
To avoid overly aggressive conditions and subsequent damage to the combustion chamber walls, the mixture ratio

$$MR = \frac{\dot{m}_{LOX}}{\dot{m}_{CH4}} \tag{2.2}$$

describing the mass ratio of oxidizer to fuel, should not exceed 4. This is mainly relevant for the limits of the operational range, as all working points are at lower mixture ratios.

2.3. Working points

LUMEN is designed with nine work points at three chamber pressures and three mixture ratios. These chamber pressures are 40 bar, 60 bar, and 80 bar, while the mixture ratios are 3.0, 3.4, and 3.8. The viability of these working points will be evaluated, though most of the analysis will focus on the main nominal working point of 60 bar and mixture ratio 3.4. The working points of other pressures represent a throttling capability from 58% to 133% nominal thrust. The working points of other mixture ratios provide a variety of operating conditions, demonstrating highly fuel-rich and close to stoichiometric operation, as the theoretical stochiometric ratio is 4.0.

3. Improvements of the digital model

As the existing digital model does no longer correctly reproduce the recently collected data, it had to be adapted. Only once the model predicts existing data correctly, its predictions can be considered reliable. Main targets of this work were the improvement of the previously used simplified valve models, and the modification of the heat flow due to the change in flame anchoring.

3.1. Valve model

For LUMEN, two main types of valves were used. Fast acting shutoff valves that can only toggle between open and closed position, and check valves that can be controlled to open to a certain portion. Their position is encoded through a number between 0, for a fully closed valve, and 1, for a fully opened valve. As the shutoff valves act sufficiently fast and are not used for the control of the engine, their modeling does not have a major impact on the engine's start-up dynamics. The check valves though are actively controlled, and their dynamic behavior can lead to oscillations and altered dynamics of the engine, especially for the start-up sequence. Correct modeling of their reaction to control signals is thus paramount.
As comparative data, a series of short square wave signals ranging from 0.4 Hz to 5 Hz was used as input to gather the real system's response at various frequencies. The results are shown in Figure 3.1. At frequencies above 0.8 Hz the system's response is no longer aligned with the control commands, as the frequency exceeds the valves capabilities. This is caused by inertia, leading to slow turn arounds as the control signal flips. This behavior also has to be reproduced by the valve's model.

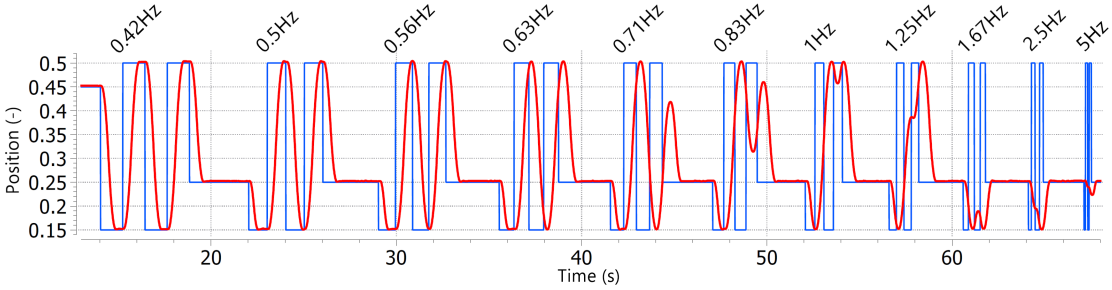

Figure 3.1.: **Response of real valve (red) to control input signal at various frequencies (blue) as indicated above**

The original valve modeling, as seen in Figure 3.2, allows instantaneous direction changes, implying a lack of inertia. This leads to a more controlled response in the old model, which instantly adjusts its direction and thus always moves towards the control signal. This incorrect modeling originates from its control method, where the valve is controlled by adjusting the speed dependent on the control error.

The first step to reach an improved valve model is to include an upper limit for the acceleration, to model inertia in combination with the torque limits of the motor. This results in an acceleration-controlled model of the valve. Although this allows for discontinuities in the third derivative, it is assumed to not be detrimental to the overall model.

The acceleration, which controls the valve, has to be modeled in such a way that the resulting valve state in the model mimics the real value. The control of the system has to preempt the sign change of the control error. Otherwise, if the acceleration for the valve control would be chosen purely based on the sign of the control error, it would lead to undampened over-swings. As such, it would continue accelerating, reaching zero control error with the highest speed, only then decelerating afterwards. This behavior is not present in the real valve. Therefore the deceleration is based upon the remaining distance relative to the current speed. In combination with accelerating towards the target whenever there is no deceleration, this keeps the distance to the target position barely larger than the stopping distance. Mathematically this is achieved by defining a potential function dependent on the target distance and speed, which smoothly transitions between 0 and 1 for states in which the system needs to accelerate and decelerate respectively. The potential function

$$p(d, v) = \frac{1}{\left(\frac{c_1 * d + 0.01}{v^2}\right)^{10} + 1} \tag{3.1}$$

with d as the deviation between current position and control signal, the current speed v, and a constant c_1 is chosen for this model. c_1 increases and decreases the "aggressiveness" of the tracking, allowing higher speeds at a given distance, leading to higher overshooting

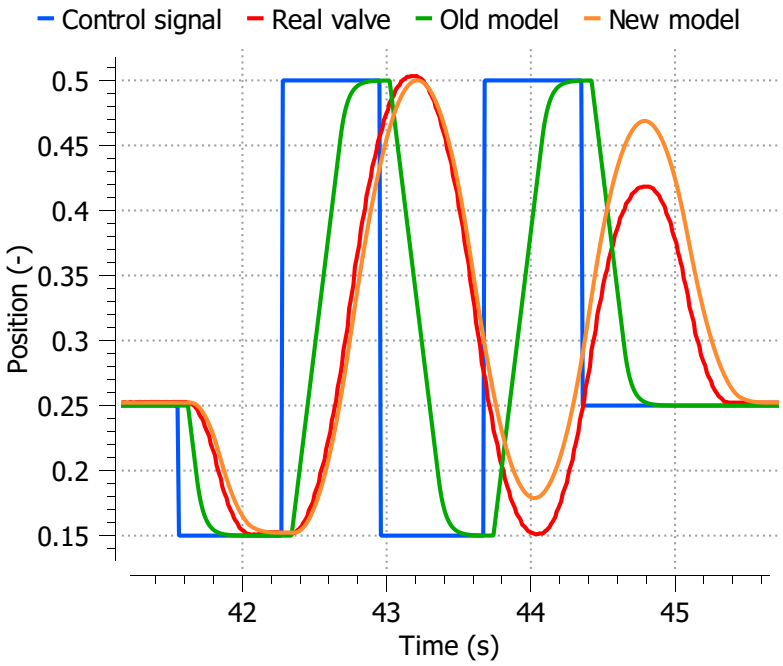

Figure 3.2.: **Valve position for a given control signal (blue). In red the real valve, in green the original model, in orange the improved model. Through a periodic control signal the frequency response of the different models is analyzed**

in favor of faster arrival. The exponent was set at 10, though any even exponent larger than 2 produces acceptable results with minor variations. A small constant, 0.01 here, is added to induce small over-swings. These are small enough to not impact the broader model, but prevent an asymptotic approach. The potential function is shown in Figure 3.3 with c_1 set to 1.

$p(d, v)$ is used in equation 3.2 to calculate the acceleration controlling the valve model. The chosen control scheme results in the valve accelerating to high speed when the deviation d to the target position is high. Once the deviation decreases below a certain point, the acceleration reduces, changing into an increasing deceleration, up to a point where the target distance stays constant relative to the stopping distance. During this, the target distance continues to shrink, until the target is reached. This matches the measured valve behavior well.

Convergence to the target is initially achieved by an asymptotic approach, since the slower the valve is moving, the less deceleration is applied. The small constant added to the deviation in the potential function makes the valve maintain a speed slightly above zero. This results in the approaching valve crossing the target, leading to a small oscillation around

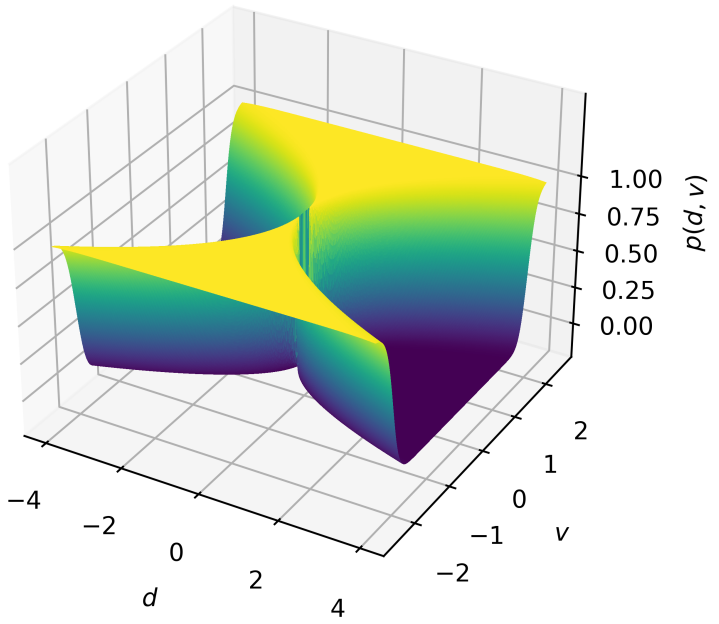

Figure 3.3.: **Potential function governing valve deceleration as given in equation 3.1 with** $c_1 = 1$

it. This oscillation is small enough to have no significance to the overall behavior.
The acceleration of the valve is given by

$$\ddot{\bar{x}} = (sgn(d) \cdot (1 - p(d, v)) - sgn(v) \cdot p(d, v)) \cdot a_{max} \tag{3.2}$$

with $sgn()$ as the sign function and a_{max} the maximum acceleration. The first half describes the acceleration term towards the target, while the later half describes the deceleration term against the current speed.
Through adjustment of the maximum acceleration, and the begin of deceleration, represented by the width of the potential function, the behavior of the new model can be adapted to closely mimic the observed real behavior. Detailed analysis however shows asymmetric behavior and a steady state error of the real valve. These can be mimicked by the model by adding artificial constant offsets to the position and velocity inputs. With these adjustments the model is a near perfect fit at lower frequencies, and maintains similar behavior at higher frequencies. There persists a notable difference to the measured value at frequencies around 0.8 Hz, as can be seen in Figure 3.4. However further adjustments of the parameters to mitigate this lead to increased errors at other frequencies.

One problem that still needs to be addressed is the limitation of the valve position to values

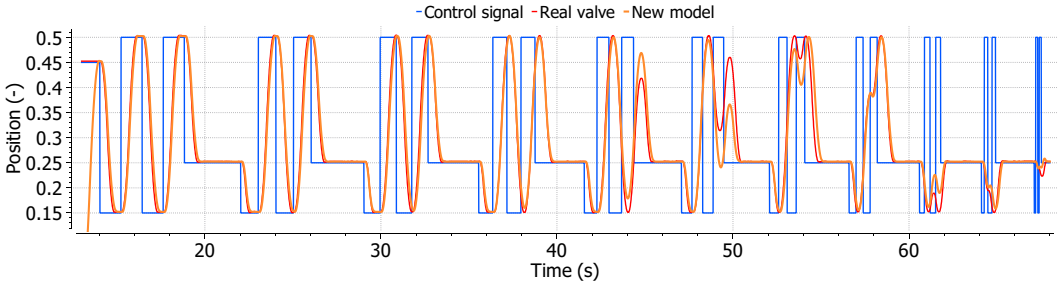

Figure 3.4.: **Response of the real valve (red) and improved model (orange) to the full test control signal (blue). Frequencies identical to Figure 3.1**

between 0 and 1. As the physical restrictions of a real valve do not apply, a model without further modifications could overshoot beyond the extreme values. To prevent this, the approach to the maximal and minimal position also needs to be anticipated. This is achieved in a similar way to the approach to a target point, targeting to keep the valve at least 5% away from the end of the range. While this makes the model inaccurate when operating at the extreme positions, these are not desired during dynamic operations, and thus not relevant.

3.2. Heat flow

One of the main results from the recent TCA-22 test campaign was the discovery of altered flame anchoring compared to previous tests, leading to an increased heat-flux into the coolant. This has to be reflected in a revised model of the engine. To evaluate the increased heat flow, the increase in internal energy of the coolant, or enthalpy, in the model has to be matched to the increase in the measured data. Enthalpy, besides the thermal energy, also includes the energy needed for phase transition and similar effects. The change in enthalpy

$$dH = C_p dT + \left(V - T \cdot \left(\frac{\partial V}{\partial T} \right)_p \right) dp \tag{3.3}$$

derives from two parts. The change in thermal energy is equal to the change in temperature dT times the heat capacity C_p of the material at constant pressure. The change in internal energy from phase transitions and expansion or compression is equal to the volume V, corrected for thermal expansion, times the pressure change dp. As the total increase in enthalpy per time is not directly measurable, it is instead is calculate through the increase

of the specific enthalpy, meaning the enthalpy per unit mass, and the mass flow rate. The mass flow rate is measured directly through flow meters. The specific enthalpy is estimated at the inlet and the outlet of the combustion chamber's cooling channels by measuring temperature and pressure. The results of the original and improved model alongside the derived thermal power are listed in Table 3.1. The measured data will be published in a separate work. While outlet conditions of the combustion chamber did not fully stabilize during the test, they were sufficiently close to a steady state to be representative.
The calculated thermal power absorbed by the combustion chamber cooling was significantly higher than the original model predicted. Through adjustment of the combustion chamber parameters, conditions closer to the measured data were achieved.

Table 3.1.: **Conditions in the chamber cooling channels**

		Old model	New model
Pressure (bar)	Inlet	110.6	110.8
	Outlet	102.6	98.2
	Δp	8.0	12.6
Temperature (K)	Inlet	130.6	130.6
	Outlet	324.0	461.2
	ΔT	193.4	330.6
Mass flow (kg/s)		1.88	1.85
Integral heat flux (MW)		1.52	2.25

Calculating the enthalpy increase, equating to the heating power, across the nozzle extension resulted in just around 140 kW, significantly below predicted values. This is likely due to the non-stabilized condition at the nozzle, as the temperature and pressure had still not reached a steady state towards the end of the test. As such, the heat flow model of the nozzle was not modified.
As this also influenced the models start-up sequence, adjustments were made to allow the model reach a steady state with the altered heat flow.

4. System Analysis

To better understand the system as a whole and its reactions to control inputs, a general analysis of the relations between the different variables is needed. The most significant and relevant connections will be highlighted in this chapter.
To get a proper overview, a large number of valve combinations were simulated, and the results gathered. As a measure to reduce complexity, BPV was not used for this initial assessment. The remaining valves' positions were chosen randomly for each sample. Additionally, more samples were generated with a focus on particular valve positions, aiming to increase available samples in key regions. However, this wide distribution of points across configuration space should be representative of the overall behavior of the engine, as any arbitrary point is likely to be similar to neighboring points that were simulated.
In total 201005 points were simulated of which 29861 conform to all constraints. This spread can be seen in Figure 4.2a, showing all simulated points, though no points with a mixture ratio above 5 or pressure below 20 bar are shown to allow for a better overview. Shown in Figure 4.1 are the distributions of valve positions across the data samples. These are not uniform due to the additional focused samples and certain valve configurations not yielding a convergent solution from the model.

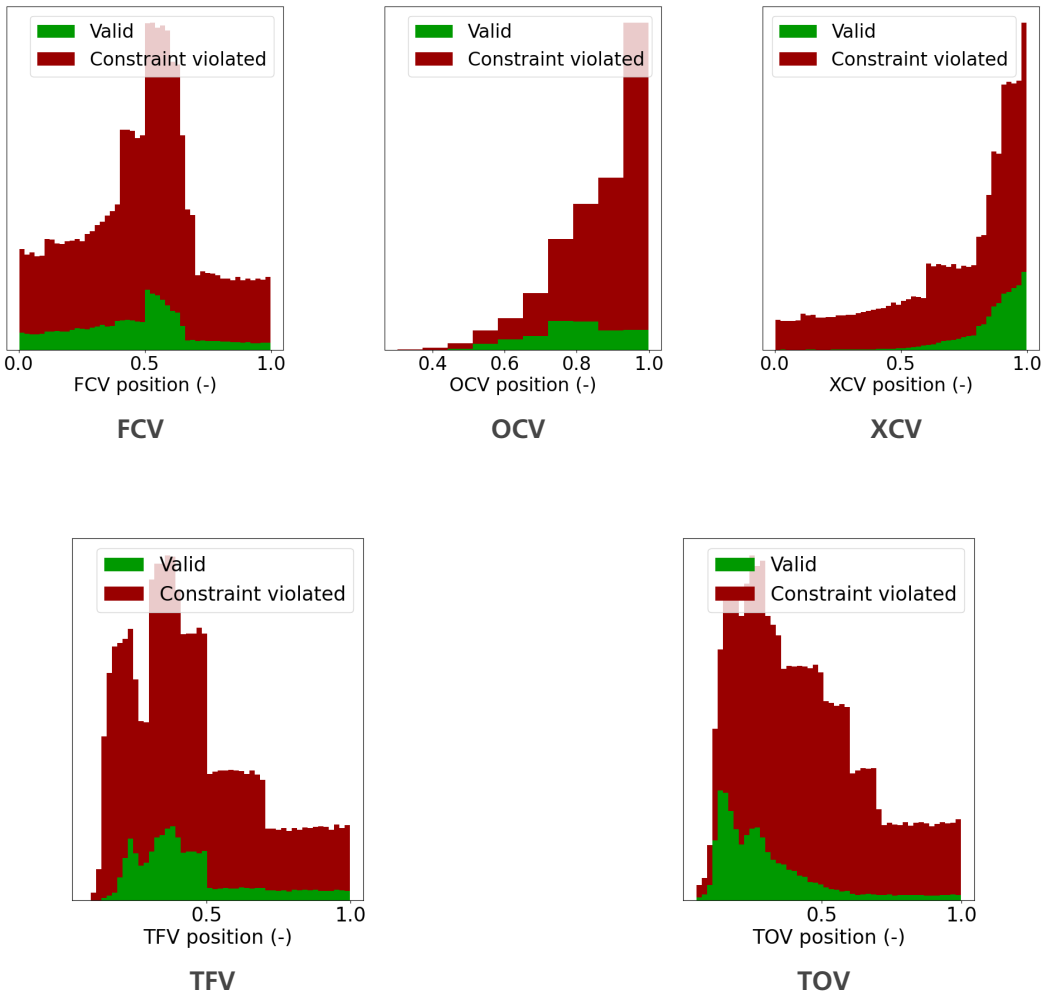

Figure 4.1.: **Valve position distributions**

4.1. Operational range

Identifying the operational range is one of the most relevant aspects and behaviors for any engine. This especially holds true for engines like LUMEN which aim for a large operational range. This includes firstly validation of the reachability of all desired working point and secondly the quantification of the remaining margins, alongside identifying what causes those limits, informing future improvements.
The general range can be seen in Figure 4.2b, reaching from 20 bar to 85 bar, and allowing

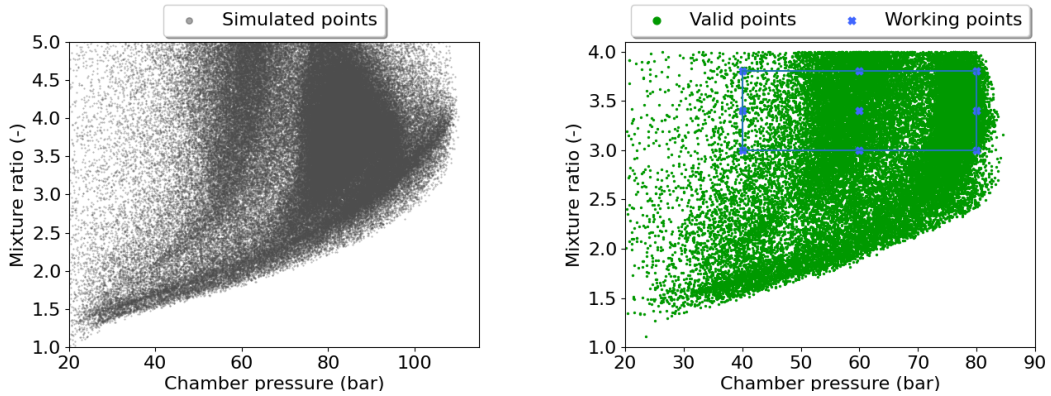

(a) **All simulated points below mixture ratio of 5 and pressure above 20 bar**

(b) **All constraint-conforming points and working range**

Figure 4.2.: **Overview of simulated operating range**

for mixture ratios as low as 1.25. The region of interest however surrounds the working points, focused on pressures of 30 bar to 90 bar, and mixture ratios ranging from 2.5 to 4. The spread of constraint-conforming points in this region shows that the vast majority of this area is accessible and all working points are reachable.

However, what is also important, are those sections that aren't accessible and the boundaries to them. In Figure 4.3 the two major types of constraint violations are highlighted. The highlighted points are ones that only violate the J or pump pressure constraint respectively, and thus would be valid if the constraints were removed or relaxed. This shows how the operational range towards higher pressures is majorly impacted by these constraints. J is critical for high and low mixture ratios, while the pump pressure is an issue for all mixture ratios. For expansion into higher pressure regimes, or for more flexibility in this region, it would thus be advantageous to improve these constraints primarily.

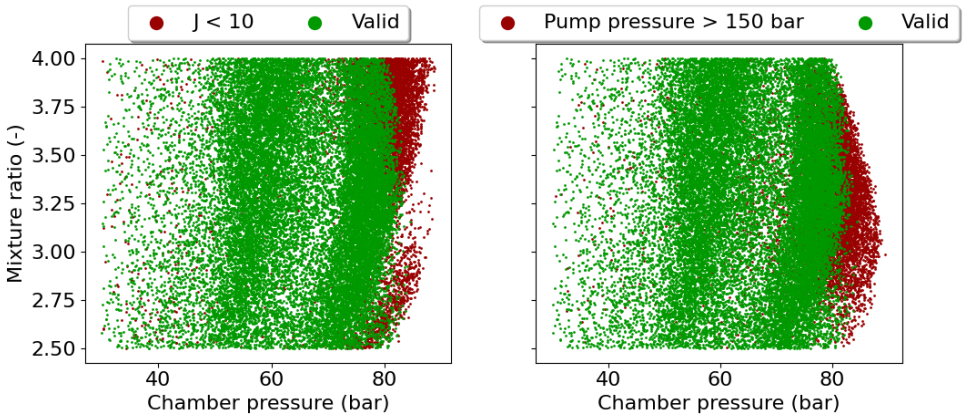

Figure 4.3.: **Points removed only due to J (left) or pump pressure (right) constraints**

With both of these constraints removed, the engine's operational range could be expanded even further, as no other constraints prohibit the operation at up to 100 bar. This can be seen in Figure 4.4, highlighting the points that only violate the pump pressure and J constraint. To reach a chamber pressure of 100 bar, the pump pressure would have to be allowed to reach 175 bar, raising the limit by 25 bar. Stable flame anchoring would have to be achieved with J as low as 3. The relation of these two variables to the chamber pressure can be seen in Figure 4.5.

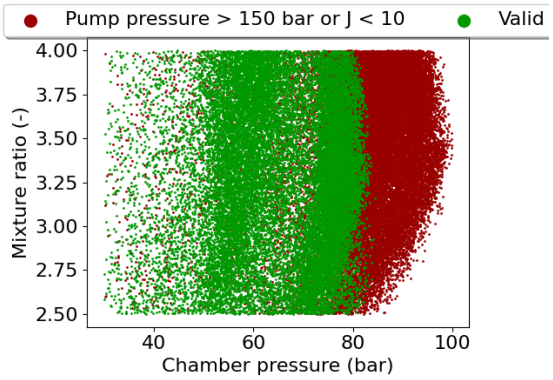

Figure 4.4.: **Valid points (green) and points at which J or pump pressure constraints were violated (red)**

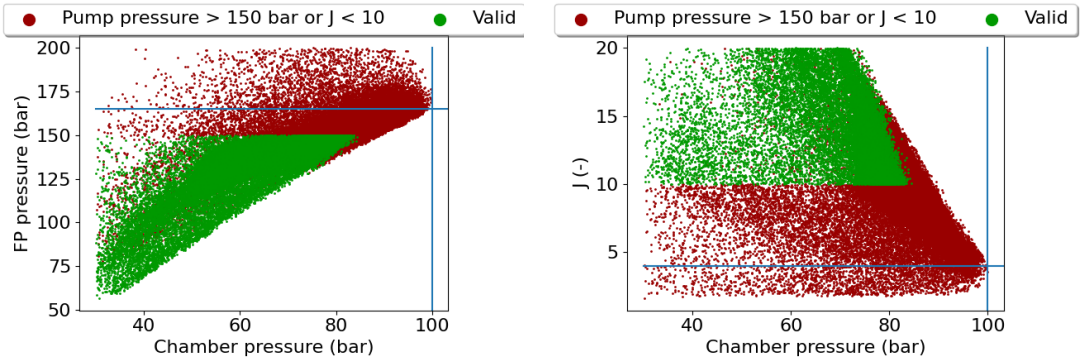

(a) **Fuel pump pressure required for certain chamber pressures**

(b) **J in relation to the chamber pressure**

Figure 4.5.: **Importance of J and pump pressure constraints on valid points for chamber pressures at different fuel pump pressures (a) or J numbers (b)**

Shown in figure 4.6 on the left is the most obvious boundary of a mixture ratio above 4.0. While operation in this area could be possible if this constraint was removed or altered, it is not desirable due to the increased oxidation damage to the combustion chamber. Also the achievable chamber pressure can not be increased by this measure.
On the right side of Figure 4.6 the constraint of critical OTP speed, implemented to avoid resonances in the oxidizer turbopump, can be seen. It forms a slightly diagonal line between around 40 bar and 50 bar chamber pressure. This region however is fully covered by valid points as well, implying that the critical speed can be avoided without impacting the operational range. Thus, the relaxation of this restraint would not extend the operational range of the engine. The same holds true for the minimum cooling mass flow and low turbine gas temperature constraints that aren't shown here. Violations of the low turbine gas temperature constraint are mainly found throughout the lower pressure regions below 30 bar, only barely extending into the regions being investigated here.

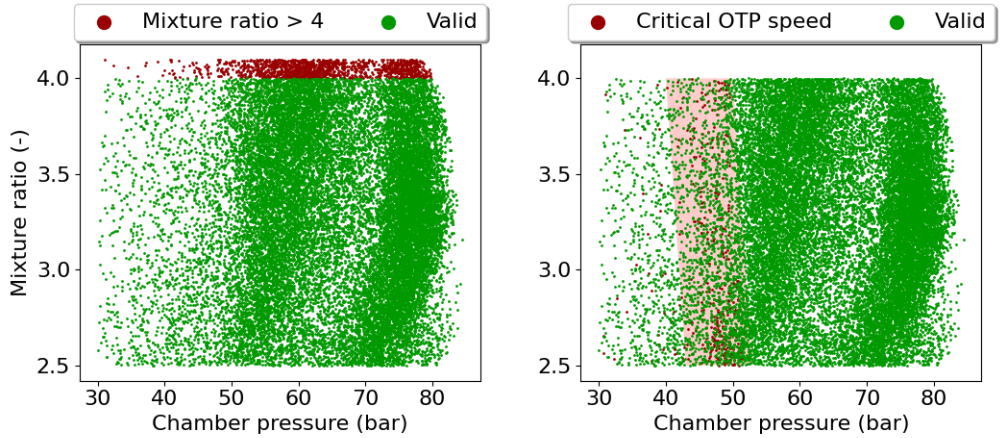

Figure 4.6.: **Points removed only due to mixture ratio (left) and critical OTP speed (right) constraints**

4.2. General

In the following the behaviors of the engine will be highlighted, that arise independent of the working point and are still apparent when allowing any chamber pressure and mixture ratio. Points that violate constraints will be included in red to provide context and show the overall behavior of the engine independent of constraints.

The I_{sp} in the following plots is normalized, with 1 being the maximum achievable I_{sp}.
As explained in section 1.1, this specific impulse is used to measure the efficiency of a rocket engine. Following the definition, specific impulse can be increased by increasing the thrust or decreasing the total mass flow. While this is valid in isolation, through the dynamics of the engine the trend over the entire operational range shows an increase in efficiency both for an increase in thrust as expected, but also for an increase in mass flow, as it can be seen in Figure 4.7.
This can be explained as a higher propellant flow also leads to higher thrust, counteracting the loss of efficiency. Higher propellant flow also increases the chamber pressure, leading to a higher exit velocity as equation 1.4 shows. This increases the efficiency further, leading to an overall increase.
The bleed mass flow is exhausted from the turbines and does not contribute to thrust generation. Thus it could be assumed that a reduction of it may increase the overall efficiency. However, the highest efficiency can be reached for a medium bleed mass flow, as seen in Figure 4.8.

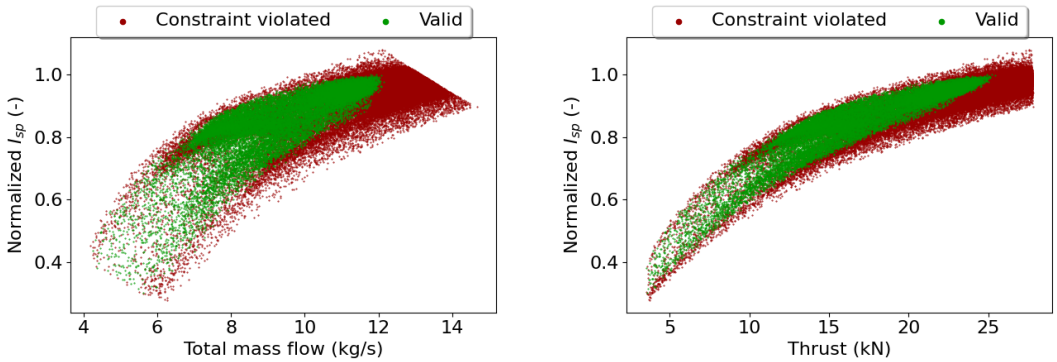

Figure 4.7.: **Dependency of I_{sp} on total mass flow and thrust across all samples**

The reason is the use of the bleed mass flow to power the pumps. Higher bleed mass

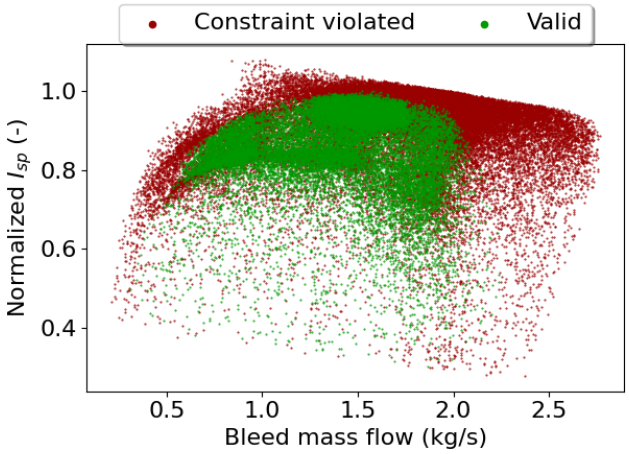

Figure 4.8.: **Dependency of I_{sp} on bleed mass flow**

flow allows higher pump pressures and subsequently higher chamber pressures. This again counteracts the mass loss, meaning that an increase in bleed mass can increase the overall efficiency up to a certain amount.
For a given pump power reducing the bleed mass flow to the turbine requires a temperature increase of the provided propellant to maintain total energy provided. This dynamic can be seen in Figure 4.9, as an increased efficiency and consequently reduced bleed mass flow necessitates higher turbine temperatures. This reaches closer to the maximum allowed turbine temperature of 700K.
Increasing the turbine temperature requires an increased temperature of the coolant up-

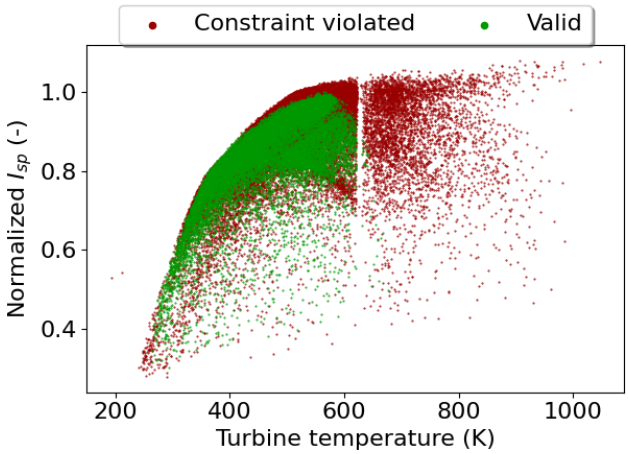

Figure 4.9.: **Dependency of I_{sp} on turbine gas temperature. The reason for the gap at 650K is unknown, but likely originates from the turbine model**

stream. Due to this, very similar dynamics can be observed for the coolant temperature of the combustion chamber coolant outlet with respect to the normalized I_{sp}.
The increase in coolant temperature may be assumed to lead to an increase in fuel injection temperature, however the simulated data only partially supports this. Figure 4.10 shows a subtle increase in injection temperature with increasing specific impulse, but also a sharp line of decreasing injection temperature at higher specific impulse. This line of maximum achievable temperature at a given specific impulse can be explained through the connection between specific impulse and chamber pressure.
As mentioned before, an increase in specific impulse and chamber pressure requires a higher propellant mass flow. An increased mass flow requires more power to reach a certain temperature, as well as more pump power to supply the propellant. The supply of propellants through the turbopumps requires a certain minimal amount of power, if all components are run as efficiently as possible. The remaining heating power from the cooling channels can be used to heat the propellant. The temperature reached this way is the maximum temperature achievable for that chamber pressure and consequently specific impulse. Any attempt to increase heating power for the propellant would decrease propellant flow and chamber pressure.
The temperature however can always be lowered, to a certain extent, as the turbines can be supplied with excess power which is later lost through inefficiencies in the system configuration.

Because J is directly linked to injection density and thus temperature, it is similarly connected to the specific impulse and chamber pressure. Similar to the maximum injection temperature

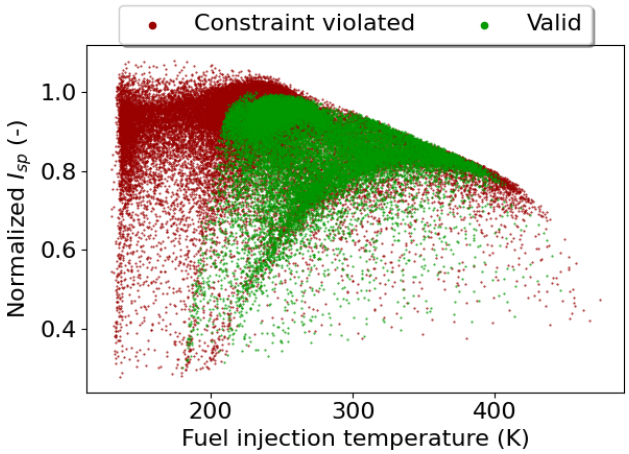

Figure 4.10.: **Dependency of I_{sp} on fuel injection temperature**

there is a maximum momentum flux ratio J achievable for any specific impulse. As the injector necessitates a minimum J of 10, these two limitations eventually meet, limiting the maximum efficiency. Alterations to the J constraint would consequently impact the maximum efficiency.

4.3. At nominal working points

A detailed analysis of the engine operation is performed for the nominal working points. Limiting the scope to this shows different dynamics and options that arise when maintaining a working point. As it removes some degrees of freedom, more variables will be interdependent.
While these behaviors change and vary with pressure, it was found that they remain largely unchanged across the mixture ratio range. As such, mainly the direct comparisons between the different pressures are important. For this, the same variables will be plotted across three plots, with each limiting the samples to those with chamber pressures around 40 bar, 60 bar, and 80 bar respectively.

By constraining the chamber pressure, the increase of efficiency through increasing the chamber pressure is no longer possible. This leads to less side influences on variables, and confirms expected behaviors. For example decreased bleed mass flow shows an increase in specific impulse, as seen in Figure 4.11. The connections established in section 4.2 remain,

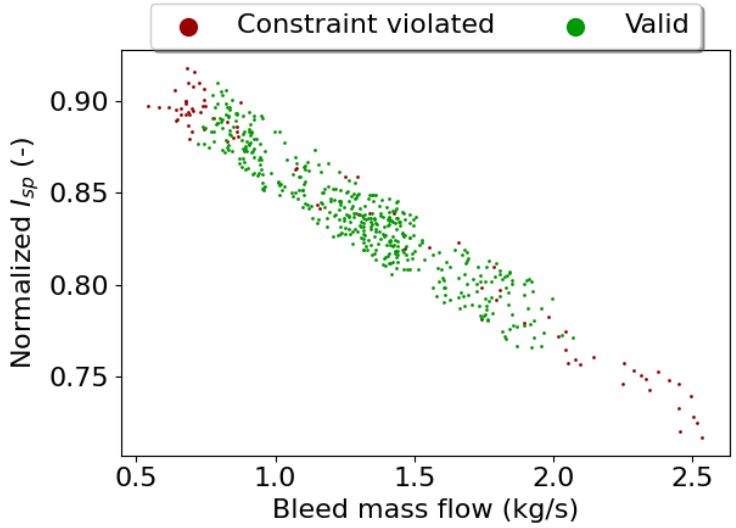

Figure 4.11.: **Dependency of I_{sp} on bleed mass flow around 60 bar chamber pressure and 3.4 mixture ratio**

Table 4.1.: **Maximum achievable J for LUMEN's working points**

Pressure (bar) / Mixture ratio	38-42	58-62	78-82
3.7-3.9	45.5	25.8	12.1
3.3-3.5	56.1	29.9	13.2
2.9-3.1	64.6	35.0	15.2

linking increasing turbine temperature to increased efficiency and increasing coolant temperature. Similarly the relationship to injection temperature gets cleared of the chamber pressure influences, leading to increasing injection temperature being linked with increasing specific impulse. Subsequently this coincides with increased momentum flux ratio J. As such, the highest efficiency is achieved at a relatively high J for each pressure range, visible in Figure 4.12.

While the correlation is weaker at higher pressures, this still means that an alteration to the J constraint would not significantly impact efficiency at any specific point. Given the impact on the operational range, a higher constraint value for J however might leave some working points impossible to achieve. This would mainly be the working points at 80 bar, as these have the lowest maximum J of all work points. The maximum J achievable for each work point is listed in Table 4.1.

This also shows the low margin for the 80 bar working points, reinforcing J as one of the

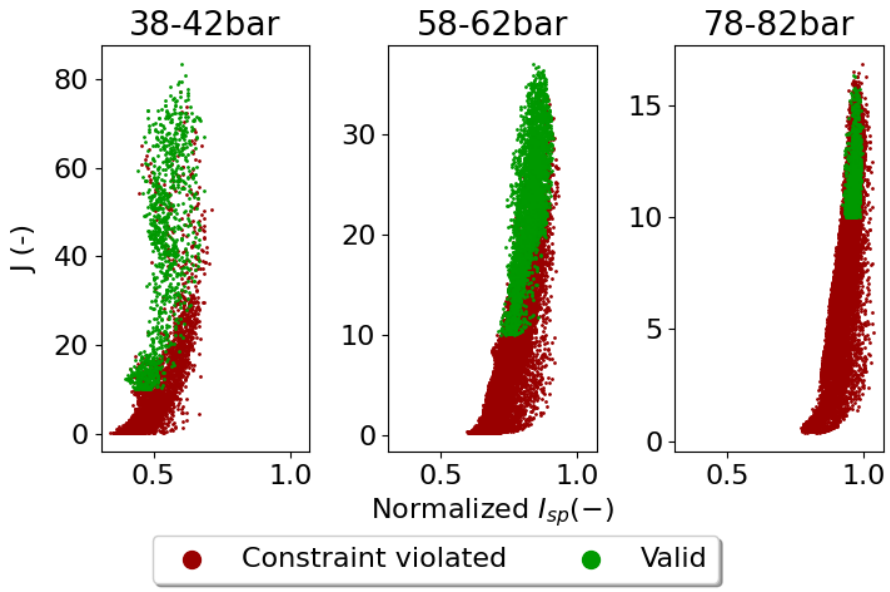

Figure 4.12.: **Dependency of momentum flux ratio J on I_{sp} at varying pressures**

Table 4.2.: **Maximum achievable relative I_{sp} for LUMEN's working points**

Mixture ratio \ Pressure (bar)	38-42	58-62	78-82
3.7-3.9	0.656	0.893	0.985
3.3-3.5	0.669	0.911	0.992
2.9-3.1	0.666	0.913	0.989

main limitations for the operational capability of LUMEN. With a minimum momentum flux ratio of 10 and maximum of 12 to 15, the operating flexibility is severely reduced, allowing for less diverse operation.
Nonetheless, the J constraint is not the limiting factor for increasing efficiency at a working point. The minimum cooling mass flow, despite not being impactful for the general operational range, limits the specific impulse. As highlighted in Figure 4.13, an increase in efficiency correlates with a decrease in chamber cooling flow, until the lower limit of this is reached. This holds true for all working points. The reason for this is twofold, as the cooling mass flow splits into two flows downstream. One is the previously mentioned bleed mass flow. A decrease in this for increased efficiency also causes decreased cooling mass flow. The other portion is the fuel that flows through XCV to be injected into the chamber. This path requires more pump power than the more direct path through FCV, as flow through the cooling channels causes a significant pressure drop. Thus a decrease in this mass flow

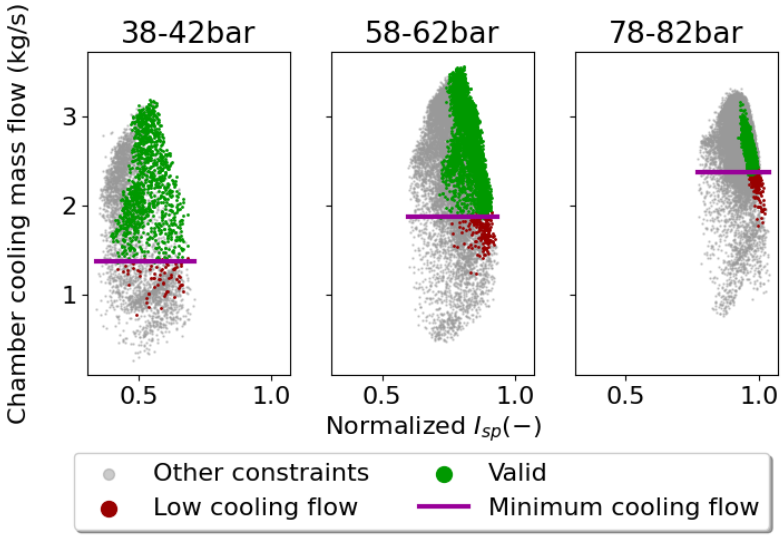

Figure 4.13.: **Dependency of chamber cooling mass flow on I_{sp} at varying pressures**

reduces the needed pump power, further raising efficiency.
This shows that the minimum cooling mass flow is the singular constraint limiting efficiency at the work points, and a decrease in this requirement would allow for a higher specific impulse.

The mixture ratio is not impactful for most quantities, mainly impacting the propellant quantities as expected. It also has an impact on J, as an increased mixture ratio lowers the maximum J possible. This is caused by the increase in oxidizer injection pressure and decrease in fuel injection pressure needed to adjust the propellant ratio. This in turn necessarily decreases J by its definition in Equation 2.1, as shown in Figure 4.14.

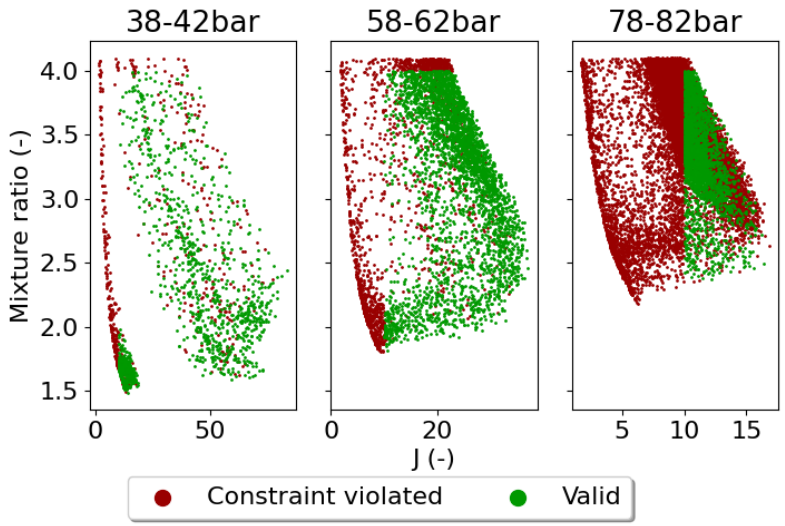

Figure 4.14.: **Dependency of mixture ratio on momentum flux ratio** J **at varying pressures**

4.4. Injection Temperature

While it is not a hard constraint, and was therefor not covered previously, a lower injection temperature is desirable for the longevity of the injection system. Ideally the fuel should be injected close to 250K. As the oxidizer temperature can not be altered by the engine, it will not be analyzed.
Studying the effects of the injection temperature on the operational range in Figure 4.15, it can be seen that all operating points are still reachable when limiting temperatures to range from 240K to 260K. The working point at 80 bar with a mixture ratio of 3.0 is on the borderline. However colder injection temperatures are less problematic. Very few samples exist around 40 bar, and a noticeably decreased number around 60 bar, indicating that this injection temperature limitation significantly limits the operational flexibility at working points of lower pressure.
As J is directly related to the injection temperature, selecting a certain desired injection temperature also selects a certain momentum flux ratio for each working point. Table 4.3 lists these for an injection temperature close to 250K. J decreases with increasing chamber pressure and mixture ratio when the injection temperature is fixed, as can be seen in Figure 4.16.

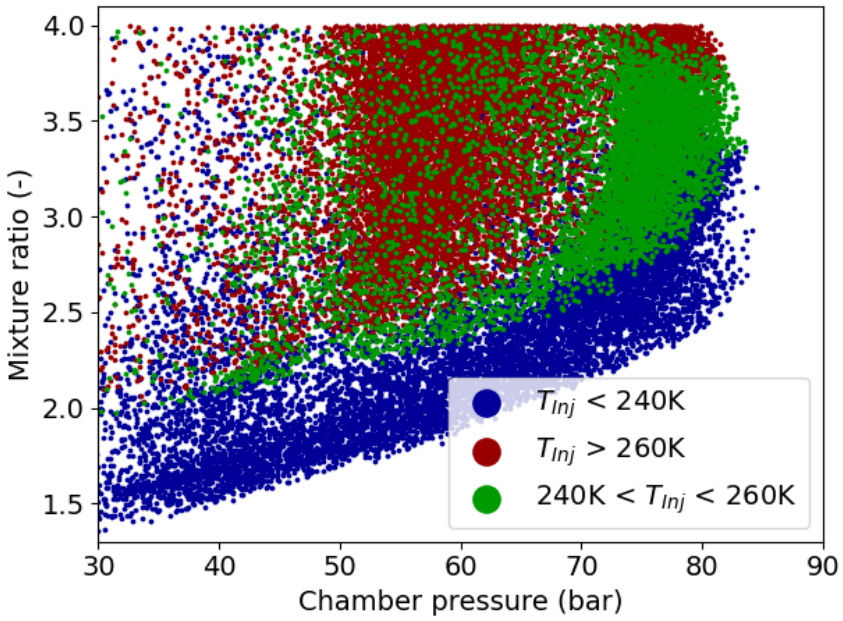

Figure 4.15.: **Operating range at varying fuel injection temperature ranges**

Table 4.3.: **Momentum flux ratio J with injection temperature of 250K**

Pressure (bar) / Mixture ratio	38-42	58-62	78-82
3.7-3.9	21	14	10
3.3-3.5	28	16	12
2.9-3.1	33	21	15

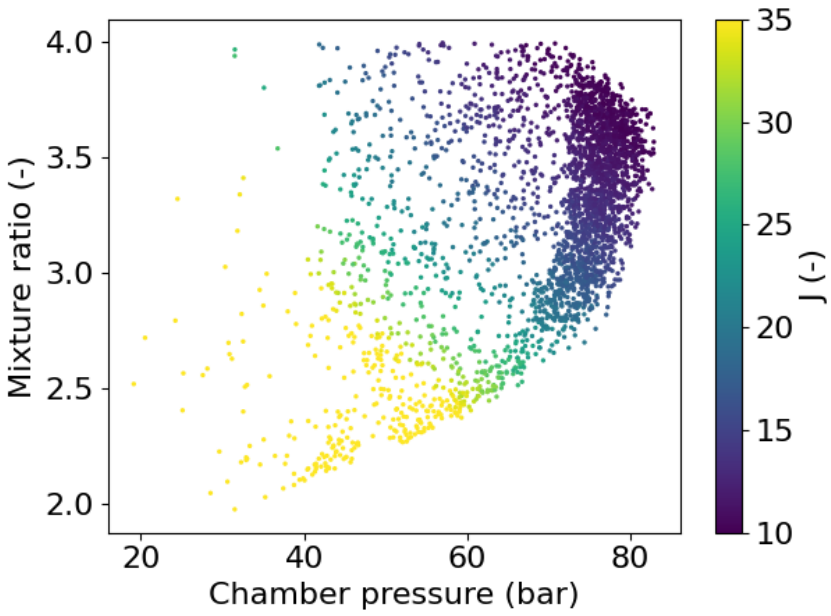

Figure 4.16.: **J across the operating range at 240K to 260K injection temperature (colorscale limited to 35)**

5. Control Analysis

Most important for the control of an engine is to understand how the possible control inputs affect the relevant control variables. For LUMEN, the possible control inputs are the positions of the five check valves, FCV, OCV, TFV, TOV, and XCV. As such, the influence these have on their own and in combination on the operation of the engine will be the focus of this chapter.
An important aspect to remember however is that correlations between a valve position and a variable aren't necessarily causal, but may be an emergent behavior from other valves compensating for the changes caused by the initial valves movement in order to keep the engine in operating parameters.

5.1. Reduced valve sets

To get a better initial overview, and limit some emergent behavior from correlated valve positions, new data generated by only utilizing a subset of the available valves is analyzed. Limiting the control options to less valves isolates the remaining valve's influence on the system more effectively. Reducing it to a single valve is however not practical, as the operational range would likely be too small for meaningful analysis, and the behavior would still depend on the chosen static positions of the other valves.
If a valve is not in the chosen set, and it isn't otherwise mentioned, it is either set fully open, for OCV and XCV, or fully closed, for FCV and BPV.

5.1.1. Turbine-controlled (TFV, TOV)

The major limitation to the operation range here is FCV being fully closed. This increases pressure drop for the fuel flow, reducing the maximum fuel flow with the available turbopump power. Thus regimes with higher fuel requirements, such as lower mixture ratios and pressures beyond 65 bar can not be reached with this configuration, as seen in Figure 5.1.

As expected, opening TFV increases chamber pressure while decreasing mixture ratio, and

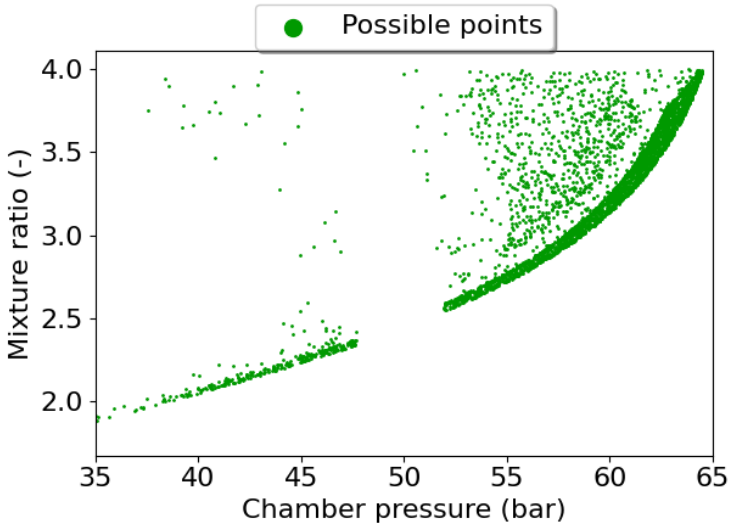

Figure 5.1.: **Operational range when varying only TFV and TOV**

opening TOV increases chamber pressure while increasing mixture ratio. This trend however does not continue up to fully opened valves. As can be seen in Figure 5.2, opening TFV beyond 0.4 or TOV beyond 0.3 results in only a minor increase in turbopump power. In the case of TFV this minor increase in total fuel flow no longer offsets the increased bleed mass flow, resulting in an overall slight drop in injected fuel. Opening of TOV increases bleed mass flow in favor of oxidizer flow either way. This behavior is not significantly altered, only dampened. This inversion of TFV's impact on the system leads to the sharp line visible in Figure 5.1, from which further opening of TFV decreases the chamber pressure, returning to previously reached points, with higher bleed mass flow.
Within the normal operating ranges of TFV and TOV however, any point of pressure and mixture ratio is only reachable by one combination of valve positions. Similarly, every point requires a set propellant flow, which has to flow through the chamber's cooling channels, as FCV is closed. The bleed mass flow, which depends solely on the position of TFV and TOV, also needs to flow through the chamber cooling channels prior. In combination this means that every point has a set cooling mass flow that can not be changed in this setup. With FCV being closed, mixing with colder fuel before injection is also not possible, leaving the injection temperature equal to the chamber coolant outlet temperature. As this outlet temperature is similarly set for each point through the cooling mass flow, the injection temperature is unable to be changed at any given point.
For operation below around 55 bar at mixture ratios above 3 only few samples are available.

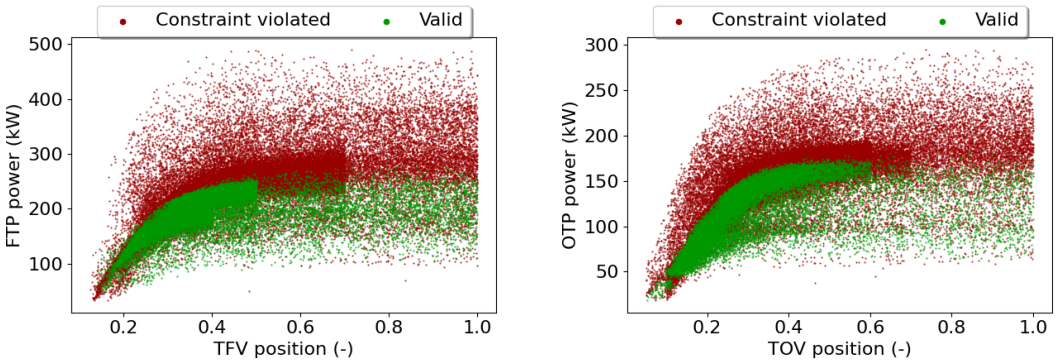

Figure 5.2.: **Limits of turbopump power depending on valve positions of TFV (left) and TOV (right)**

This hints at the model becoming numerically unstable due to too low turbine power.

Including BPV

By utilizing the bypass valve, the bleed mass flow can be further increased without altering the turbine power, and subsequently the chamber pressure or mixture ratio. This allows flexibility in the cooling mass flow, though only upwards. That in turn can decrease the fuel injection temperature, allowing injection temperatures below 300K in the entire operational range. It also stabilizes operation at low pressures. The gap around 50 bar is caused by the critical speed constraint of the OTP.

Including XCV

Using XCV in addition to TFV and TOV provides no significant benefits. Its only potential function without the usage of FCV could be altering the ratio between bleed mass and injection mass, which is done more effectively by BPV.

Varying FCV

Changing FCV to a different, but still constant position allows a shift of the operating range to higher pressures, as seen in Figure 5.3. Similar dynamics compared to the previous

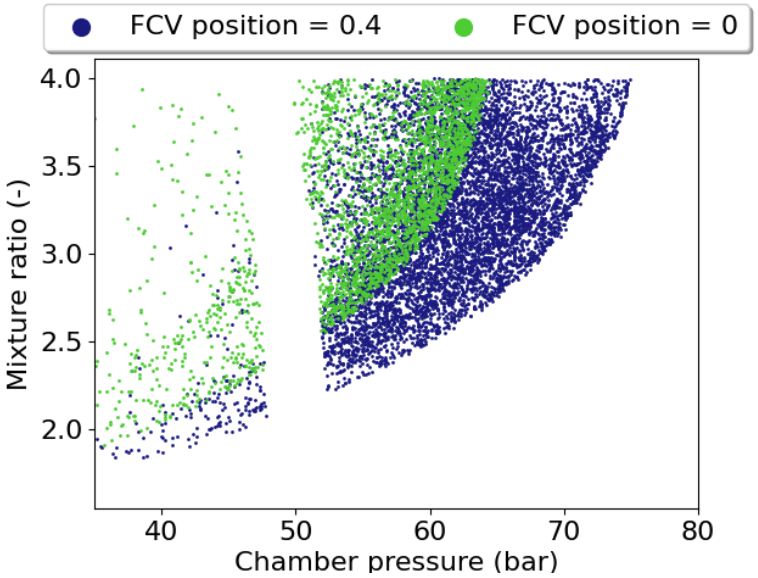

Figure 5.3.: **Comparison between fixed FCV positions 0 (green) and 0.4 (blue**

section persist regarding the usage of the other valves. The behavior does not change significantly, allowing for control of the chamber pressure and mixture ratio through TFV and TOV, with the cooling mass flow unable to be controlled independently. The lower pressure regime is less accessible, as now the onset of numerical instability is raised to higher pressures.

5.1.2. With mixer (FCV, TFV, TOV)

With FCV available, the amount of injected fuel can be increased significantly. Opening FCV routes more fuel directly to the combustion chamber, avoiding the pressure drop of the cooling channels. This also decreases pressure downstream of the cooling channels, decreasing the bleed mass flow relative to the injection mass flow. Independent control of the cooling mass flow like this allows for more efficient usage of the turbopump power. It can be used to improve specific impulse at existing points, or to reach higher chamber pressures than previously possible. This expansion of the envelope, visible in Figure 5.4, gets

close to the full operational range of the engine established in Figure 4.2b, particularly in the high pressure regions. The remaining mismatch mainly stems from insufficient samples

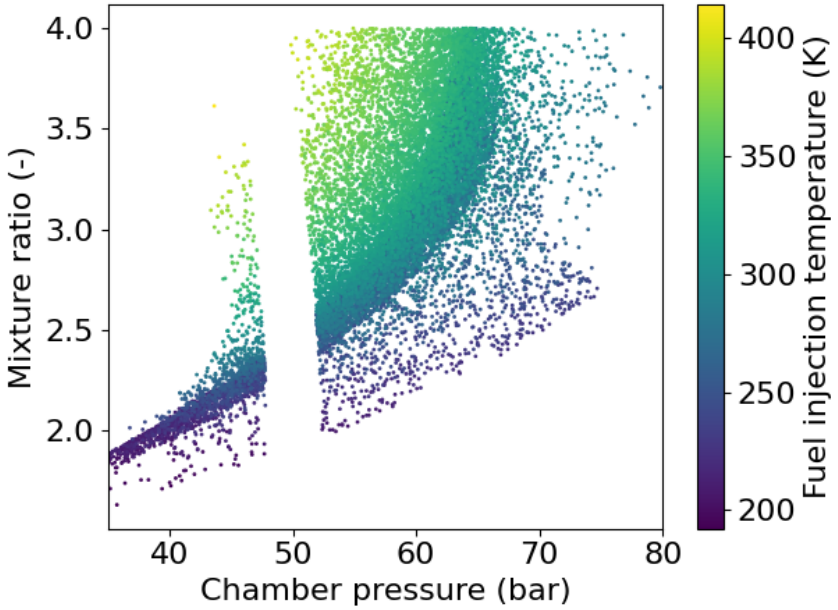

Figure 5.4.: **Operational range when varying only FCV, TFV and TOV**

in the high pressure regions, as neither closing OCV nor XCV is required for high pressure operation. This can not be said about the low pressure regions, where these two valves are critical, and as such these regions are not readily accessible when only using FCV, TFV and TOV. The OTP critical speed constraint blocks all points close to 50 bar, while even lower pressures would require throttling of the turbines to a state too low for stable operation.
Despite the independent control of the cooling mass flow, independent control of injection temperature is not the case, still depending on the chamber pressure and mixture ratio. As Figure 5.4 shows, the injection temperature increases with decreasing injection fuel mass. This can be explained by considering the flow of thermal energy at a fixed point. As the heating power of the cooling channels and the power required by the turbines is nearly constant, the difference between these is constant as well. This difference is contained in the fuel that gets added into the combustion chamber. As the mass flow is also constant, no difference in fuel routing can change its final temperature.

Including BPV

As BPV allows venting of heated fuel after the chamber cooling channels, it can also serve to get rid of unneeded thermal energy. This solves the problem of a fixed injection temperature explained in the previous paragraph. By reducing the cooling mass flow to increase its temperature, and then venting a portion of it, the injection temperature can be significantly reduced. This allows injection temperatures close to 250K across the entire operational range. Specific impulse is not significantly impacted by this mode of operation.

Including XCV

Utilizing XCV does not significantly affect the injection temperature or operational range. While reductions in injection temperature can be achieved by closing XCV to 0.6 and lower, this necessitates opening TFV beyond 0.4 to allow for additional bleed mass. This could also be done by utilizing BPV. However, BPV already enables effective control of the injection temperature without XCV, making it redundant in this context.

5.2. Control effects of valves

While the valves do not act independently of one another, and their positions aren't uncorrelated, their individual impacts on the system are still of interest. The most important influences of actuating each valve will be highlighted, together with the sensible positions of each valve.

5.2.1. FCV

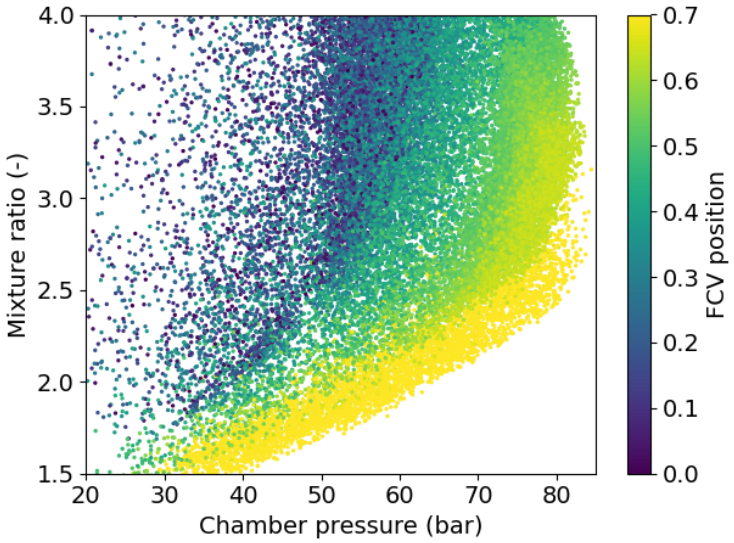

Figure 5.5.: **Position of FCV across the operational range**

FCV serves to increase the overall injection fuel flow, decreasing injection temperature and cooling flow in the process. This increased injection fuel flow increases the chamber pressure while decreasing the mixture ratio, as seen in Figure 5.5. It is not required up to chamber pressure of around 60 bar, but can increase efficiency. With FCV, and the turbine valves, almost the same range of operation points can be reached as with all valves. The full range above a mixture ratio of 3 can be reached with a FCV position between 0 and 0.6. Opening it further is only necessary for very low mixture ratios.

5.2.2. OCV

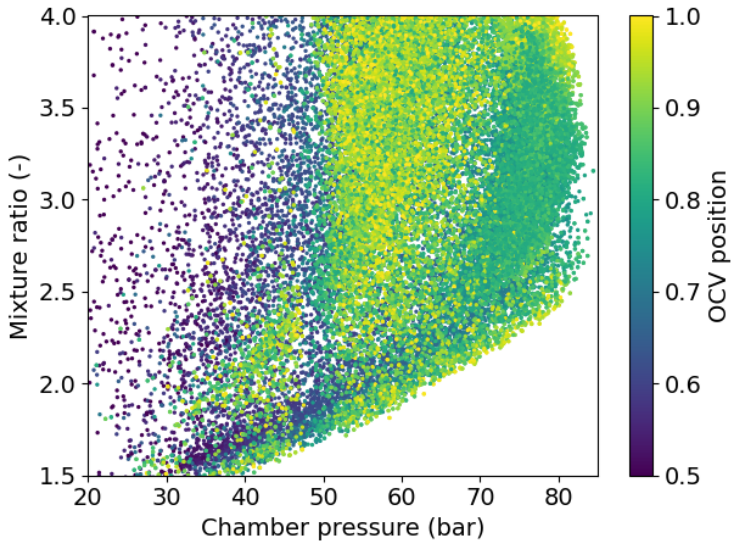

Figure 5.6.: **Position of OCV across the operational range**

OCV appears redundant for the control of oxidizer flow, which is mainly controlled through the turbopump power and thus TOV. While it is most efficient to leave OCV fully open in most situations, it is paramount in avoiding the critical OTP speed. This constraint can't be avoided around 50 bar chamber pressure when OCV is fully opened. When OCV is available, these areas can be reached by choosing an OTP speed higher than the critical speed regime, and reducing the mass flow by closing OCV, as visible in Figure 5.6. Even lower chamber pressures can also be reached more reliably through this method, avoiding numerical instability of the oxidizer turbine. OCV should remain as far open as possible to increase efficiency, but may need to be closed as far as 0.6 to reach all working points.

5.2.3. TFV

TFV controls the FTP power, increasing the bleed mass flow when opened. The increase in FTP power leads to increased fuel flow, raising chamber pressure and decreasing mixture ratio as shown in Figure 5.7. As it also increases the pressure ahead of the turbine valves, OTP power and oxidizer flow is also slightly increased. Above positions of 0.4, FTP power is only marginally increased, instead only increasing bleed mass flow. In this state TFV begins acting similar to BPV, serving as a bleed valve. As such, for nominal operation, TFV remains

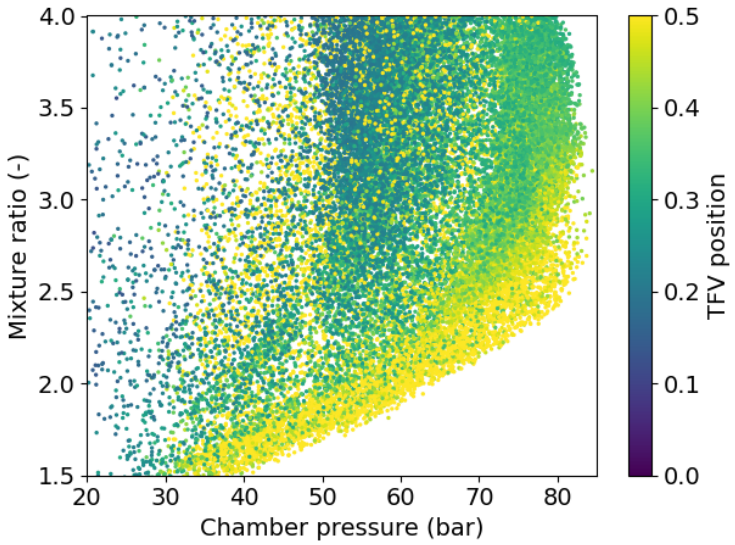

Figure 5.7.: **Position of TFV across the operational range**

between 0.15 and 0.4. Closing the valve below 0.15 leads to numerical instability of the turbine model.

5.2.4. TOV

TOV controls OTP power, increasing the bleed mass flow when opened. The increase in OTP power leads to increased oxidizer flow, raising chamber pressure and mixture ratio, shown in Figure 5.8. As the oxidizer system does not significantly interact with the more complex fuel system, TOV does not influence many other variables. Similarly to TFV, above 0.3 TOV can act as a bleed valve, not significantly increasing OTP power anymore. Numerical instabilities in the turbine appear below 0.1, leaving the nominal range of this valve between 0.1 and 0.3.

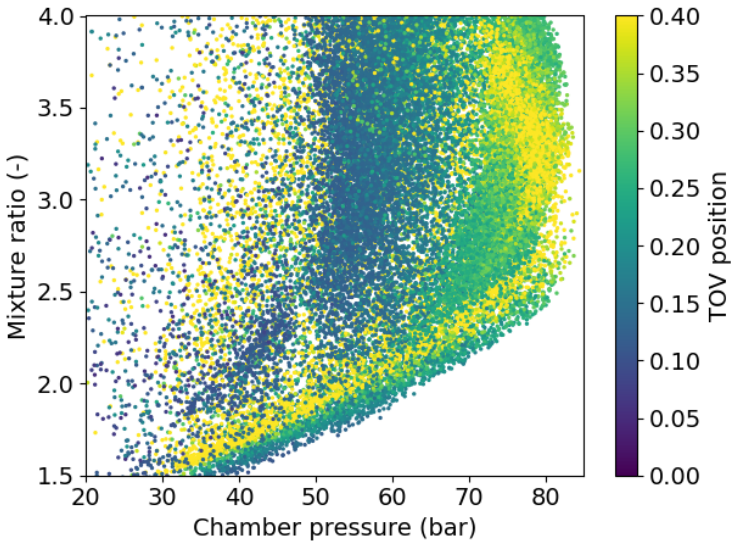

Figure 5.8.: **Position of TOV across the operational range**

5.2.5. XCV

XCV regulates the crossflow from the cooling channels to the fuel injection. This works in conjunction with FCV, enhancing each others effects by exchanging heated fuel for cold fuel when XCV is closed and FCV opened. As the required cooling mass flow is relatively high compared to needed bleed mass flow, a high mass flow through XCV is usually necessary with only a small reduction possible. This limits the range of XCV to above 0.8 in most cases. As the cooling flow requirement drops with lower chamber pressures, XCV can be closed up to 0.6 in the range of 40 bar.

5.2.6. BPV

BPV allows to decrease injection temperature further than otherwise possible. As FCV allows injection temperatures sufficiently low, BPV isn't needed in normal operation, though it increases flexibility. BPV can be operated from 0 to 1, depending on what is required.

6. Conclusion and outlook

The digital model of LUMEN was improved to match new test data. The main change was an increased heat flux into the coolant caused by altered flame anchoring. To ensure stable flame anchoring, a constraint on the momentum flux ratio was introduced alongside other operational constraints. The simulation model was used to generate data for analysis of the impact of these changes. This involved looking at the operational range and its limitations. It was determined all working points can still be reached, and that the main limitations for higher pressures are the maximum pump pressure and minimum momentum flux ratio.
Relations between variables both in general and at the fixed working points were analyzed with a focus on the specific impulse. It was found that momentum flux ratios of 12 or above can be reached at all working points, allowing for stable flame anchoring. Maximum specific impulse at a working point was found to coincide with high momentum flux ratio, meaning an increase in requirements of the flux ratio would not negatively impact efficiency.
The secondary goal of maintaining an injection temperature of 250K was evaluated. This further restriction would still allow operation at all working points with reduced momentum flux ratio as low as 10, without impacting efficiency significantly. The most significant limitation for working points was identified as the minimum cooling mass flow.
Finally, the operating range of reduced valve sets was compared, showing influences and relevance of selected valves. OCV and XCV were found to best remain fully open for chamber pressures higher than 55 bar, but are critical in lower pressure regimes. OCV is useful to avoid OTP critical speed constraints, while XCV enables lower fuel flows. FCV is needed to control fuel injection temperature and enable pressures above 65 bar. BPV, despite initial assumptions, is useful to control injection temperature instead of or in conjunction with FCV.
The findings in regard to J show that the current injector design can be maintained if a J of 10 ensures stable flame anchoring. An injection temperature of 250K, while reducing flexibility, does not significantly impact the operational range or efficiency.
Changing the injector to a different design without J constraint however would offer the opportunity of higher pressure operation. This would be even further enabled by an upgrade of the fuel side components to support pressures beyond 150 bar, which however would be very costly.

To improve performance at working points, the cooling channel and chamber geometry would have to be altered to allow for lower coolant flows.
In conclusion, regardless of these potential alterations, the current configuration of LUMEN fulfills its purpose of serving as a modular breadboard engine for research into LNG expander bleed cycles. It can stably operate at a variety of mixture ratios and chamber pressures, and can do so while reducing wear on its components.
The system analysis performed within this work gives a solid foundation for future simulation analysis and will support future test runs and design decisions.

Appendix

I. Used symbols

C_p	Heat capacity at constant pressure
C_v	Heat capacity at constant volume
d	Deviation
F_T	Thrust force
g_0	Standard gravity
γ	Isentropic expansion factor
I_{sp}	Specific impulse
J	Momentum flux ratio
M	Molecular mass
MR	Mixture ratio
$\dot{m}_e$	Exhaust mass flow
$\dot{m}_t$	Total mass flow
p	Pressure
p_e	Absolute outlet pressure

p_i	Absolute inlet pressure
$P_{kin,e}$	Kinetic energy of the exhaust
ρ	Density
R	Universal gas law constant
T	Temperature
v	Velocity
V	Volume
v_e	Exhaust velocity
v_e^*	Effective exhaust velocity

II. Abbreviations

BPT Turbine Bypass Valve
BPV Bypass Valve
CH4 Methane
FCV Fuel Control Valve
FFM Fuel Flow Meter
FTP Fuel Turbo Pump
IGN Igniter
INJ Injector
LH2 Liquid Hydrogen
LNG Liquefied Natural Gas
LOX Liquid Oxygen
MCC Main Combustion Chamber
MFV Main Fuel Valve
MOV Main Oxidizer Valve
MR Mixture Ratio
NEM Nozzle Extension
OCV Oxidizer Control Valve
OFM Oxidizer Flow Meter
OTP Oxidizer Turbo Pump
TCA Thrust Chamber Assembly
TFV Turbine(Fuel) Valve
TOV Turbine(Oxidizer) Valve
TP Turbo Pump
XCV Crossfeed Control Valve

III. References

[1] Peter Beck and Jessica Tulp. "Rocket lab: Liberating the small satellite market". In: (2017).

[2] RE BURCHAM and RB KELLER. "Liquid rocket engine turbopump rotating-shaft seals[NASA Space Vehicle Design Criteria, Chemical Propulsion]". In: (1978).

[3] ES Gall, MW McIlveen, and AL Berg. *Qualification Tests of the Apollo Block II Service Module Engine (AJ10-137)*. Tech. rep. ARNOLD ENGINEERING DEVELOPMENT CENTER ARNOLD AFB TN, 1967.

[4] GS Gill and WH Nurick. *Liquid rocket engine injectors*. Tech. rep. 1976.

[5] Bill Greene. *J-2X Progress: Current Status, The End of 2012*. 2013. URL: https://blogs.nasa.gov/J2X/tag/turbopump/ (visited on 04/23/2023).

[6] Jan Haemisch et al. "LUMEN-Design of the Regenerative Cooling System for an Expander Bleed Cycle Engine Using Methane". In: (2021).

[7] Oskar J Haidn. "Advanced rocket engines". In: *Advances on propulsion technology for high-speed aircraft* 1 (2008), pp. 6–1.

[8] John A Halchak, James L Cannon, and Corey Brown. *Materials for liquid propulsion systems*. Tech. rep. American Institute of Aeronautics and Astronautics, 2018.

[9] Horst Holsten et al. "Space Transportation Systems". In: *Handbook of Space Technology*. John Wiley and Sons, Ltd, 2009. Chap. 3, pp. 114–198. ISBN: 9780470742433. DOI: https://doi.org/10.1002/9780470742433.ch3. eprint: https://onlinelibrary.wiley.com/doi/pdf/10.1002/9780470742433.ch3. URL: https://onlinelibrary.wiley.com/doi/abs/10.1002/9780470742433.ch3.

[10] Hideto Kawashima et al. "Progress of LE-9 engine development". In: *2018 Joint Propulsion Conference*. 2018, p. 4458.

[11] A Krach and A Sutton. "Another look at the practical and theoretical limits of an expander cycle, LOX/H2 engine". In: *35th Joint Propulsion Conference and Exhibit*. 1999, p. 2473.

[12] Keming Liang, Baoe Yang, and Zhongli Zhang. "Investigation of Heat Transfer and Coking Characteristics of Hydrocarbon Fuels". In: *Journal of Propulsion and Power* 14.5 (1998), pp. 789–796. DOI: 10.2514/2.5342. eprint: https://doi.org/10.2514/2.5342. URL: https://doi.org/10.2514/2.5342.

[13] Ernst Messerschmid and Stefanos Fasoulas. *Raumfahrtsysteme*. Vol. 2. Springer, 2011.

[14] Blue Origin. *America's next rocket engine*. 2023. URL: https://www.blueorigin.com/engines/be-4/ (visited on 04/23/2023).

[15] Christian Schmierer et al. "Advancing Europe's Hybrid Rocket Engine Technology with Paraffin and LOX". In: *8th European Conference for Aeronautics and Space Sciences EUCASS*. 2019. URL: https://elib.dlr.de/130301/.

[16] Erik Seedhouse. Cham: Springer International Publishing, 2022. ISBN: 978-3-030-99181-4. DOI: 10.1007/978-3-030-99181-4. URL: https://doi.org/10.1007/978-3-030-99181-4.

[17] Erik Seedhouse. *SpaceX: Making Commercial Spaceflight a Reality*. New York, NY: Springer New York, 2013. ISBN: 978-1-4614-5514-1. DOI: 10.1007/978-1-4614-5514-1. URL: https://doi.org/10.1007/978-1-4614-5514-1.

[18] Nicole Shriver. "Combustion Tap-Off Cycle". In: (2016).

[19] Tobias Traudt et al. "Liquid Upper Stage Demonstrator Engine (LUMEN): Component Test Results and Project Progress". In: (2022).

[20] M.J.L. Turner. *Rocket and Spacecraft Propulsion: Principles, Practice And New Developments*. Springer-Praxis Bks. Springer, 2005. ISBN: 9783540221906. URL: https://books.google.de/books?id=ja1ROyh4yPYC.

[21] IOK. *Nozzle-de-Laval-diagram*. 2008. URL: https://upload.wikimedia.org/wikipedia/commons/4/4c/Nozzle_de_Laval_diagram.svg (visited on 04/23/2023).

IV. Acknowledgements

Finally I'd like to extend my thanks to all those people that have enabled me to reach this point in the first place.

First of all of course to Professor Günther Waxenegger, who recommended me for the topic of this thesis and brought me to DLR in the first place. Always encouraging and friendly, you were confident in my abilities and knowledge, making no challenge seem too great to overcome. Never one to understate the importance of the topic at hand, you were a great motivator, but were always open for a more casual chat just the same. Whether it was about the latest space news or my current lectures, it never failed to eased the mood, especially when the work wasn't panning out quite as planned. And despite machine learning not really being my favorite topic, you managed to spark my interest in it all the same.
Thank you also to Professor Jan Deeken for the review of this thesis as well as managing the LUMEN project, enabling this work in the first place. Similarly my thanks extend to all those people involved in the LUMEN project, working to realize this unique concept.
A big thanks also goes out to Kai Dresia who, alongside Günther, supervised my work, guiding and helping me when I was stuck, especially with the programs I was less accustomed to beforehand. Our weekly meetings always gave an opportunity to jointly review the progress, discuss the implications, and decide on what to do moving forward.
On a more personal note I'd like to thank all my dear friends who have always been there for me. Oftentimes helping me more indirectly throughout the years, playing games together or simply having an open ear for my problems, though especially throughout the last few months, helping take the edge off stressful or frustrating days. Some have helped more directly as well though, offering advise, proof reading tirelessly and fixing my insecurities in english grammar.
Along the same lines I can't forget my sister, who I could always turn to for advise and diversion, ranging from navigating the formalities of academia to watching funny videos together. Sharing the same passion for space, I was always happy to keep you up-to-date on space news, and together speculate about its implications. And even being on vacation didn't stop you from taking the time to proof read and offer in-depth comments and suggestions for my thesis.
Similarly my mom never shied away from giving me a helping hand when I needed one, helping me with moves, and always keeping me on track. Your passion and knowledge of computer science and math inspired me to always learn more and pursue that passion, and I hope your students find a similar spark within them.